J/ψ photoproduction amplitude analyses

Jefferson Lab
Thomas Jefferson National Accelerator Facility

OLD DOMINION UNIVERSITY

Arkaitz Rodas

Winney, et al. (JPAC) [PRD 108 (2023) 054018]

Winney, et al. (JPAC) [PRD 100 (2019) 034019]

Hiller Blin, et al. (JPAC) [PRD 100 (2016) 034002]

JPAC

EXOHAD
EXOTIC HADRONS TOPICAL COLLABORATION

J/ψ photoproduction (near threshold)

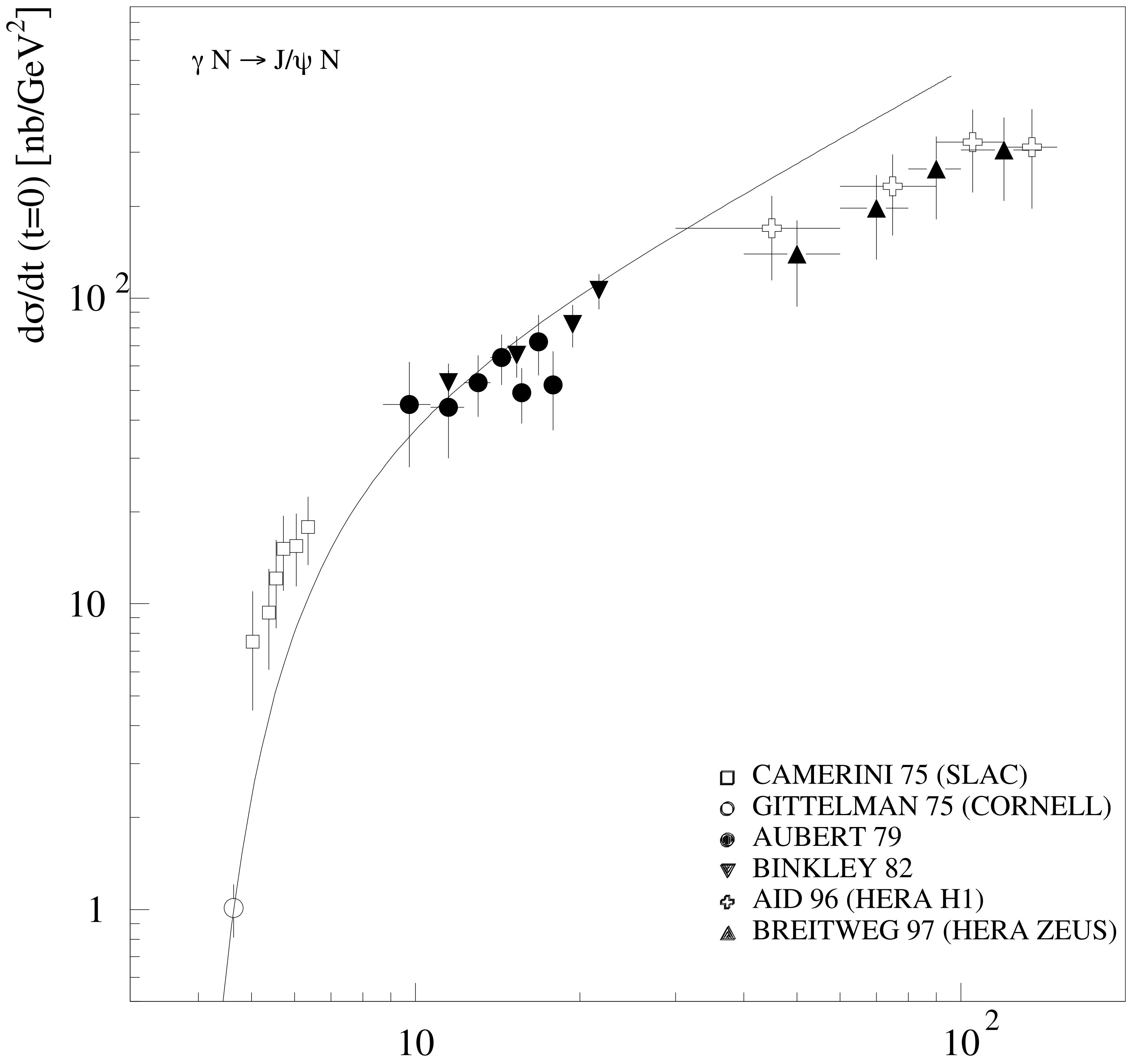

Kharzeev et al. [EPJC 9 (1999) 459]

Brodsky et al. [PLB 498 (2001) 23]

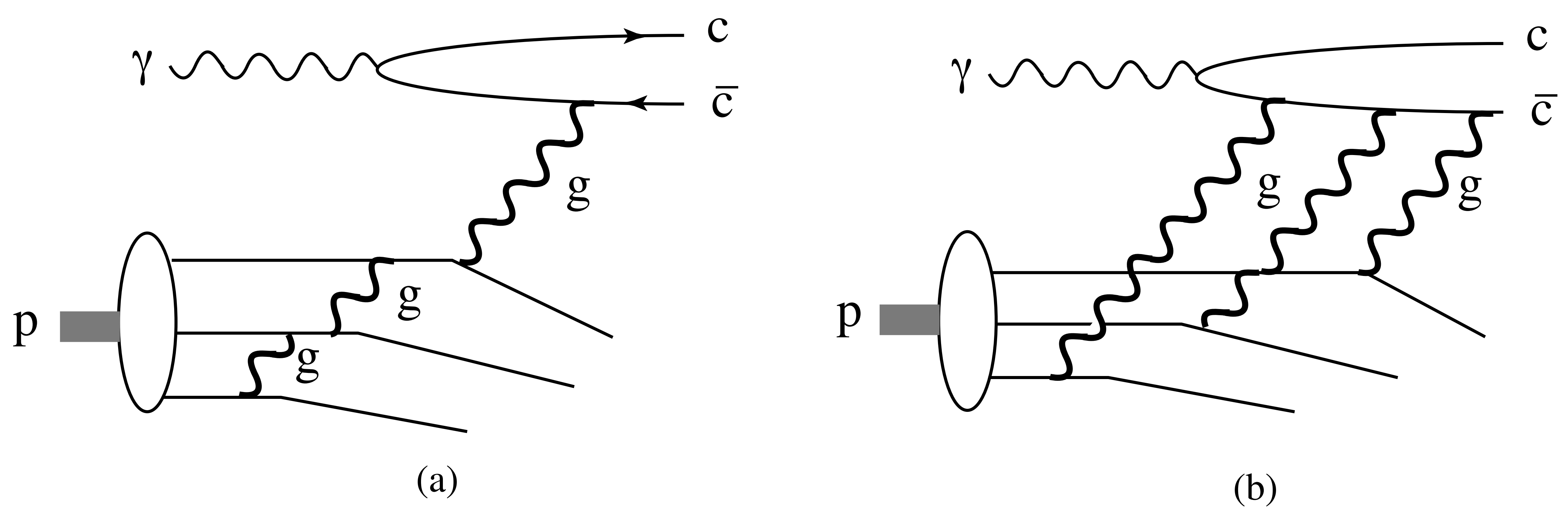

No obviously "q connected" contributing process:

- Small *J/ψ*→NN (no baryon exchanges)
- OZI suppression (no light meson exchanges)
- Heavy quark masses (no heavy meson exchanges)

"*J/ψ* probes nonperturbative gluonic distributions"

J/ψ photoproduction (near threshold)

Measurements at energies near threshold have attracted a lot of attention as potentitally sensitive to key quantities relevant to proton structure

Based on factorization arguments in perturbative and holographic QCD can be used to extract:

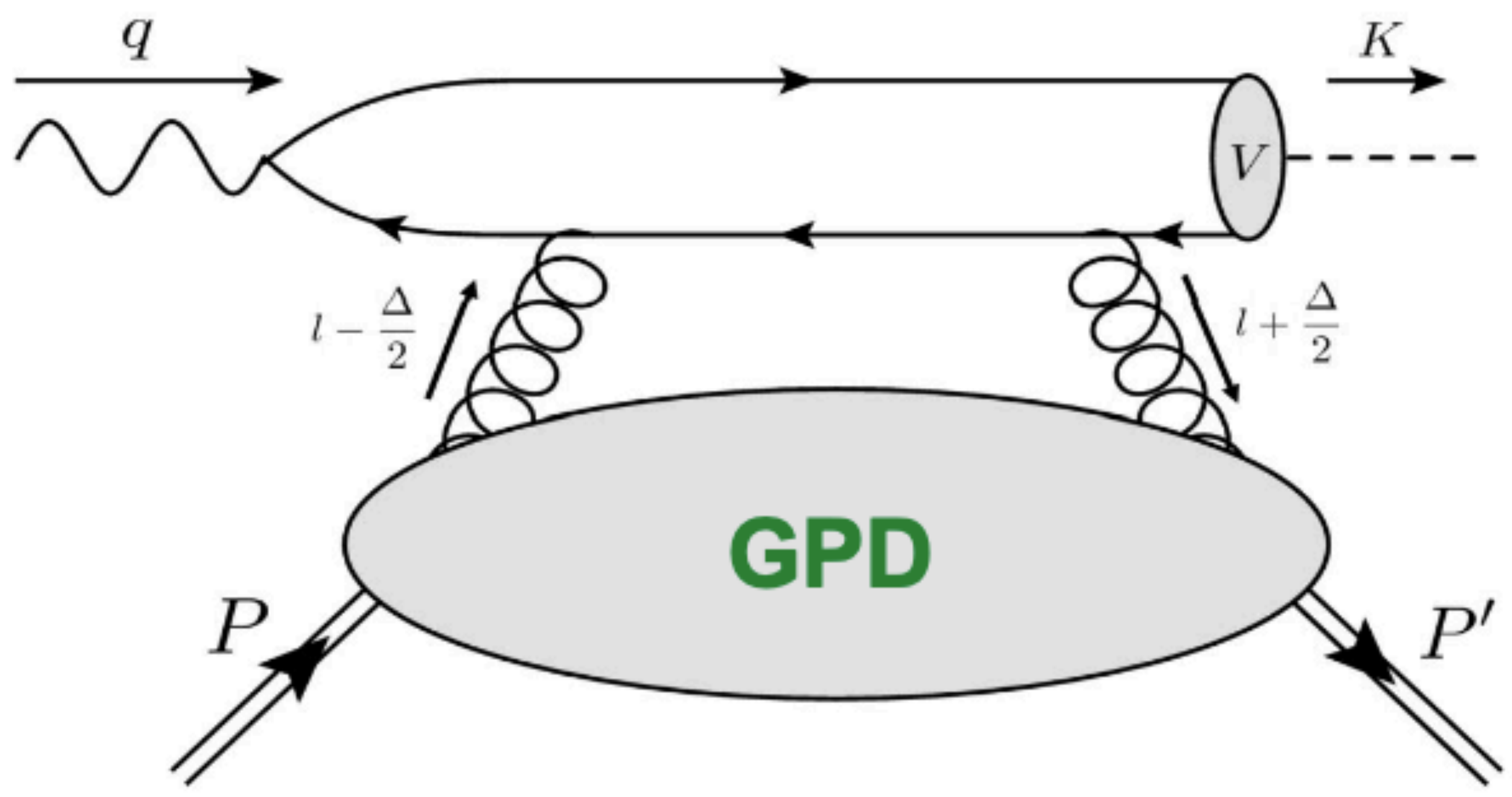

- Gravitational form factors

  Mamo & Zahed [PRD 101 (2020) 086003]
  Guo, Ji & Liu [PRD 103 (2021) 096010]

- Mass radius

  Kharzeev [PRD 104 (2021) 054015]
  Mamo & Zaheed [PRD 103 (2021) 094010]

$$\langle R_m^2 \rangle = \frac{6}{M} \frac{dG}{dt}\Big|_{t=0}$$

- Trace anomaly contribution to proton mass

  Wang, Chen & Evslin [EPJC 80 (2020) 507]
  Hatta & Yang [PRD 98 (2018) 074003]

J/ψ photoproduction (near threshold)

Measurements at energies near threshold have attracted a lot of attention as potentitally sensitive to key quantities relevant to exotic hadrons

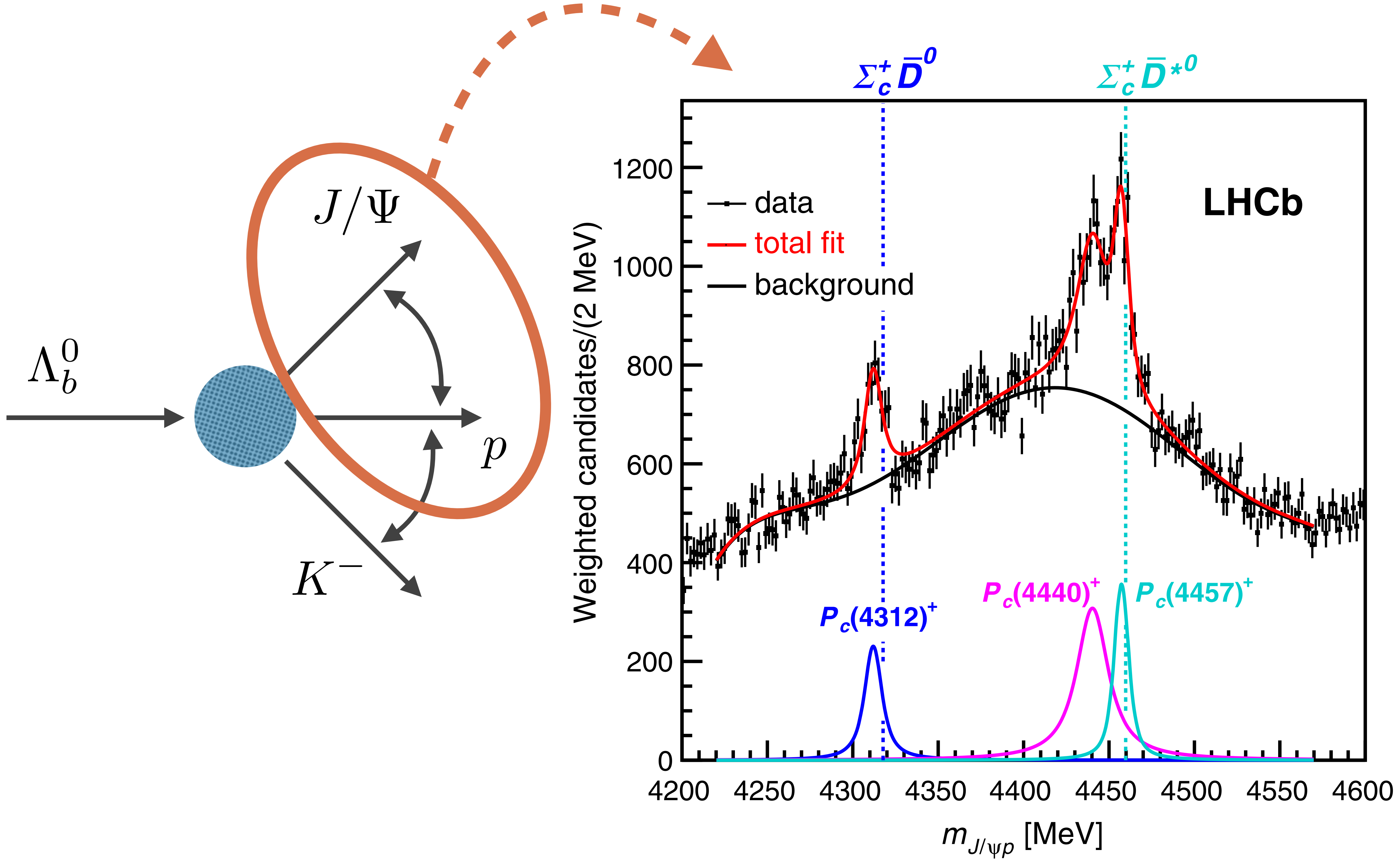

These data: LHCb [PRL 122 (2019) 222001]
Discovery: LHCb [PRL 115 (2015) 072001]

Observation of hidden charm pentaquark candidates by LHCb sparked interest in photoproduction searches

Wang et al. [PRD 92 (2015) 034022]
Karliner & Rosner [PLB 752 (2016) 329]
Hiller Blin et al. [PRD 94 (2016) 034002]

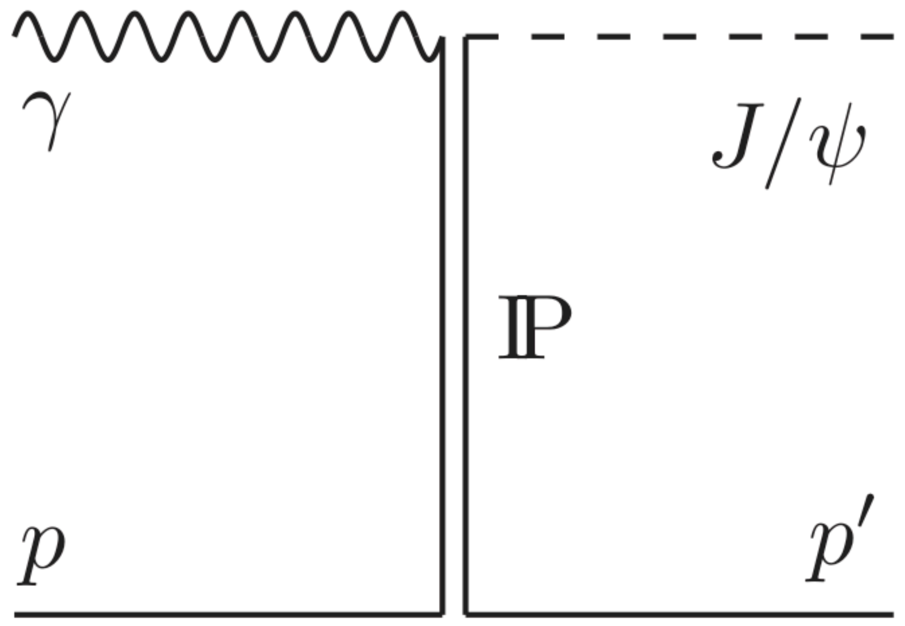

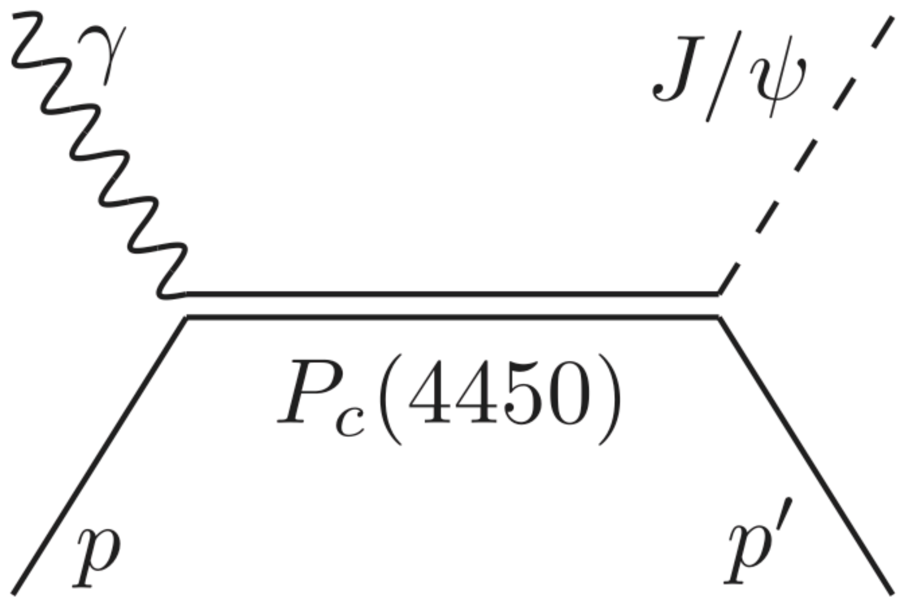

J/ψ photoproduction (near threshold)

GlueX [PRL 123 (2019) 072001]

GlueX observes diffractive scattering with no sign of pentaquarks!

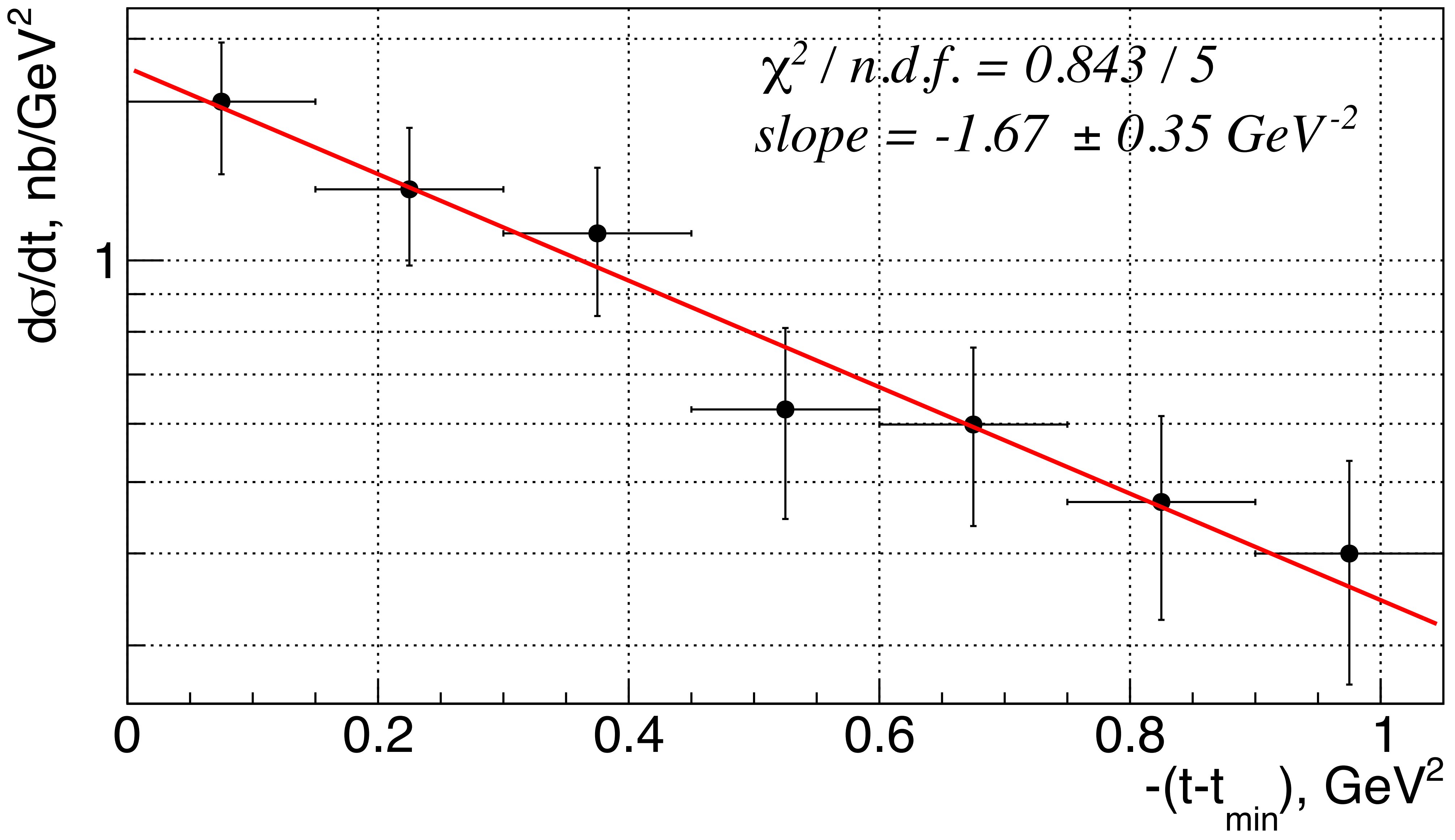

Confirmation of gluon dominated dynamics?

JPAC model: Assume P_c^+ couples with predefined strength

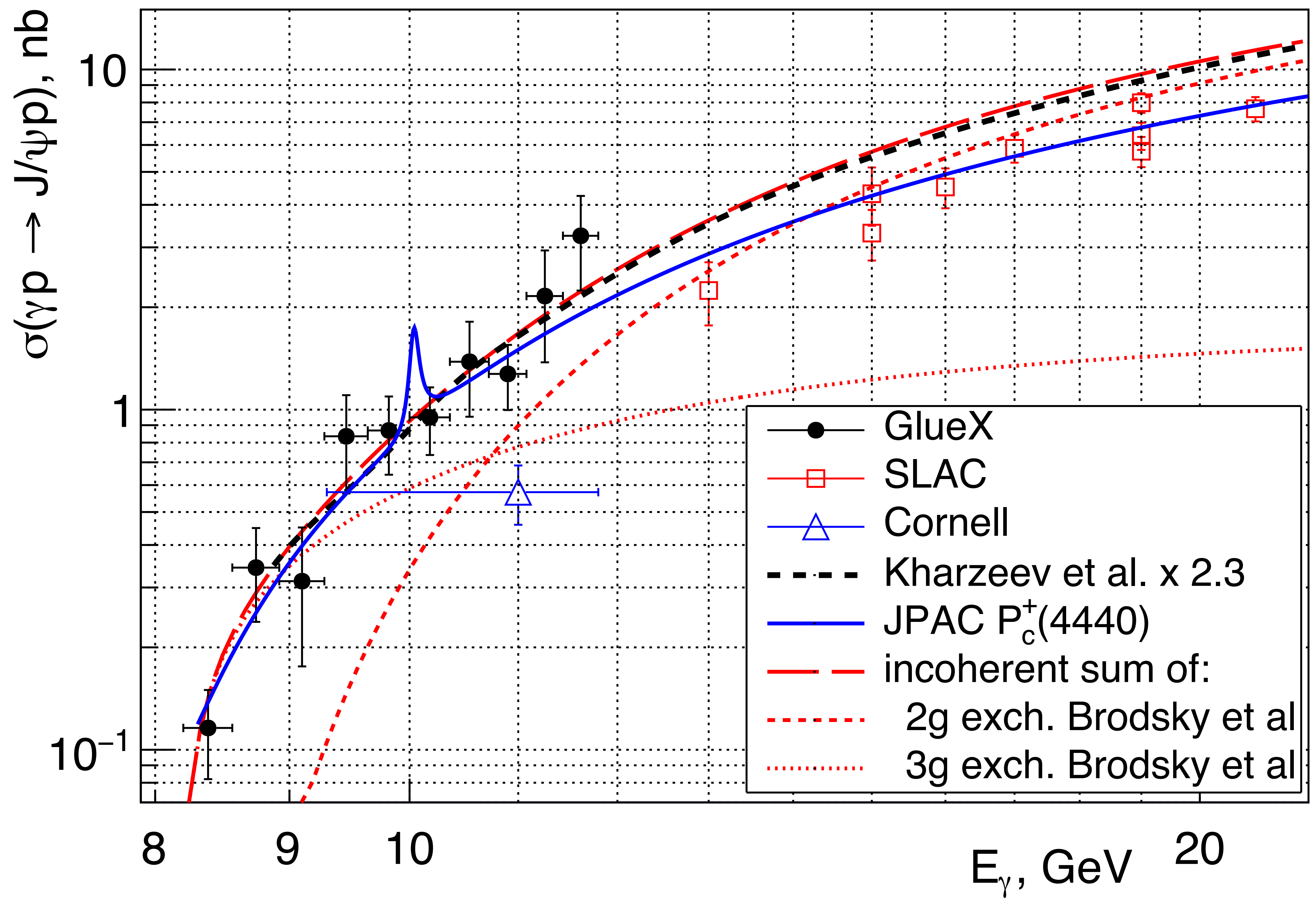

But... the cross section is not precise enough to discard them!

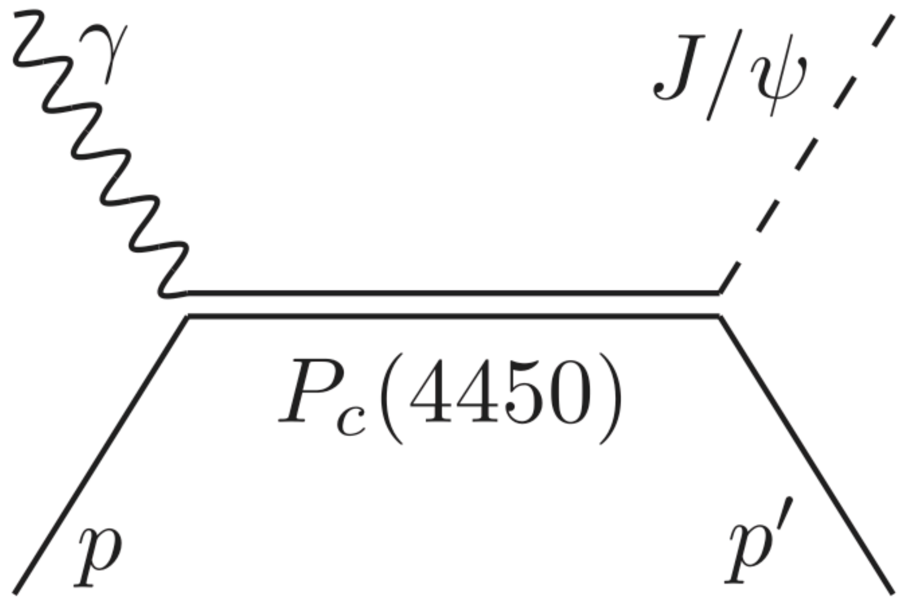

J/ψ photoproduction (near threshold)

Du et al. [EPJC 80 (2019) 1053]

Possible structure in the integrated cross section coinciding with open charm thresholds

Although kinematically suppressed, coupled channel mechanism expected to be compensated by larger photoproduction rates of open charm

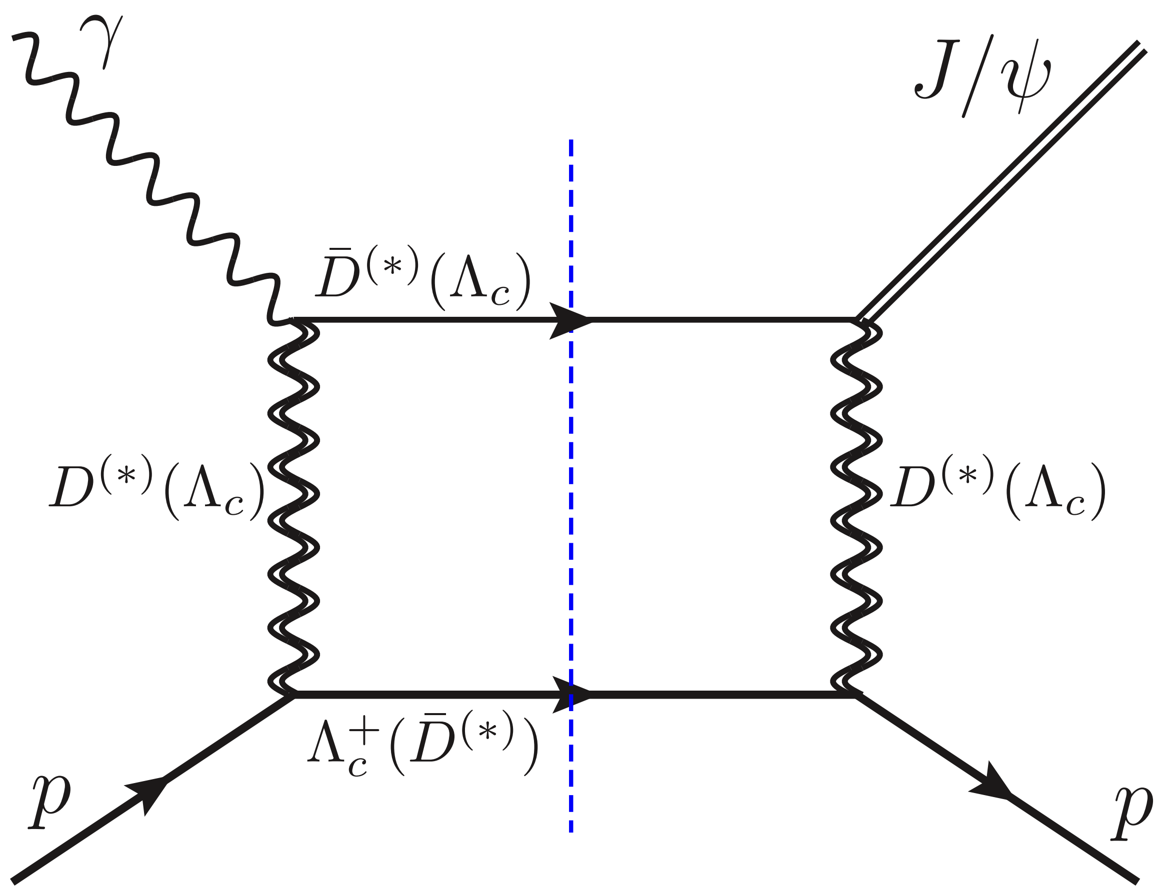

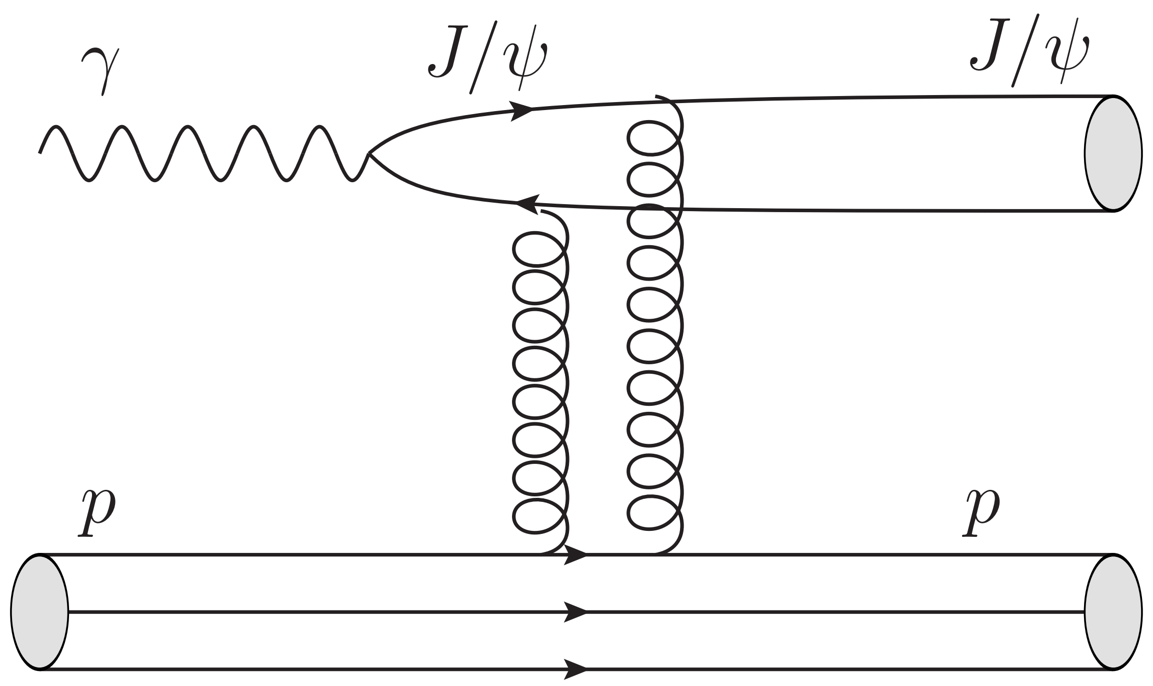

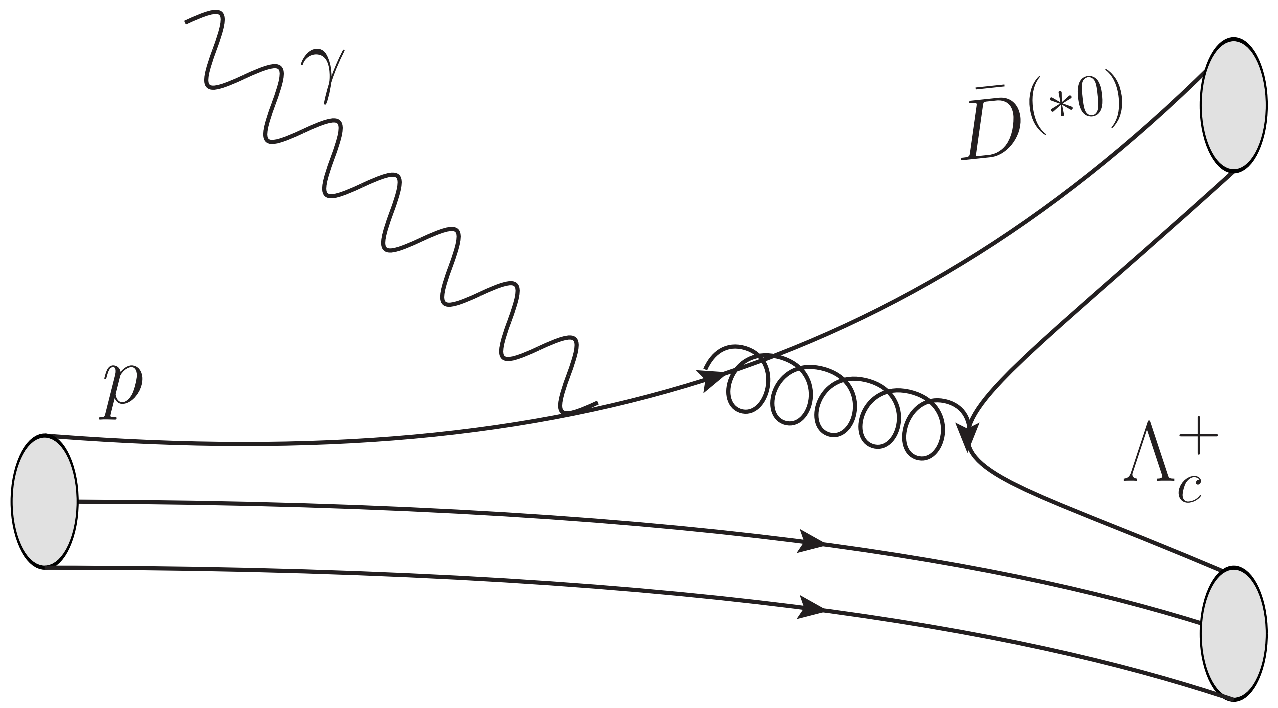

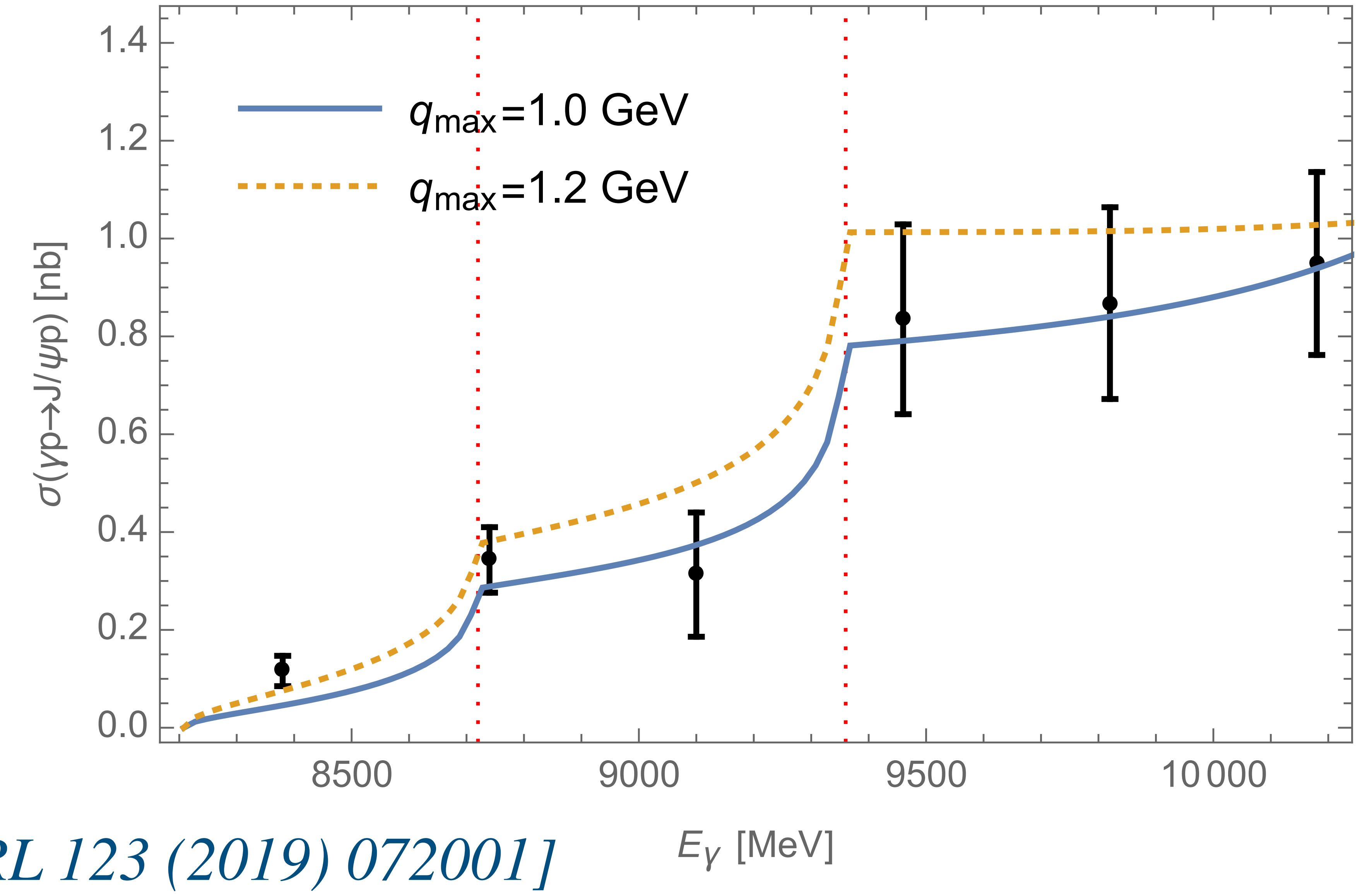

Data from GlueX [PRL 123 (2019) 072001]

Factorization

GPD approach assumes strict QCD factorization
Motivated in infinite heavy quark limit (leading order), at large skewness, and small *t*

Guo, Ji & Liu [PRD 103 (2021) 096010]

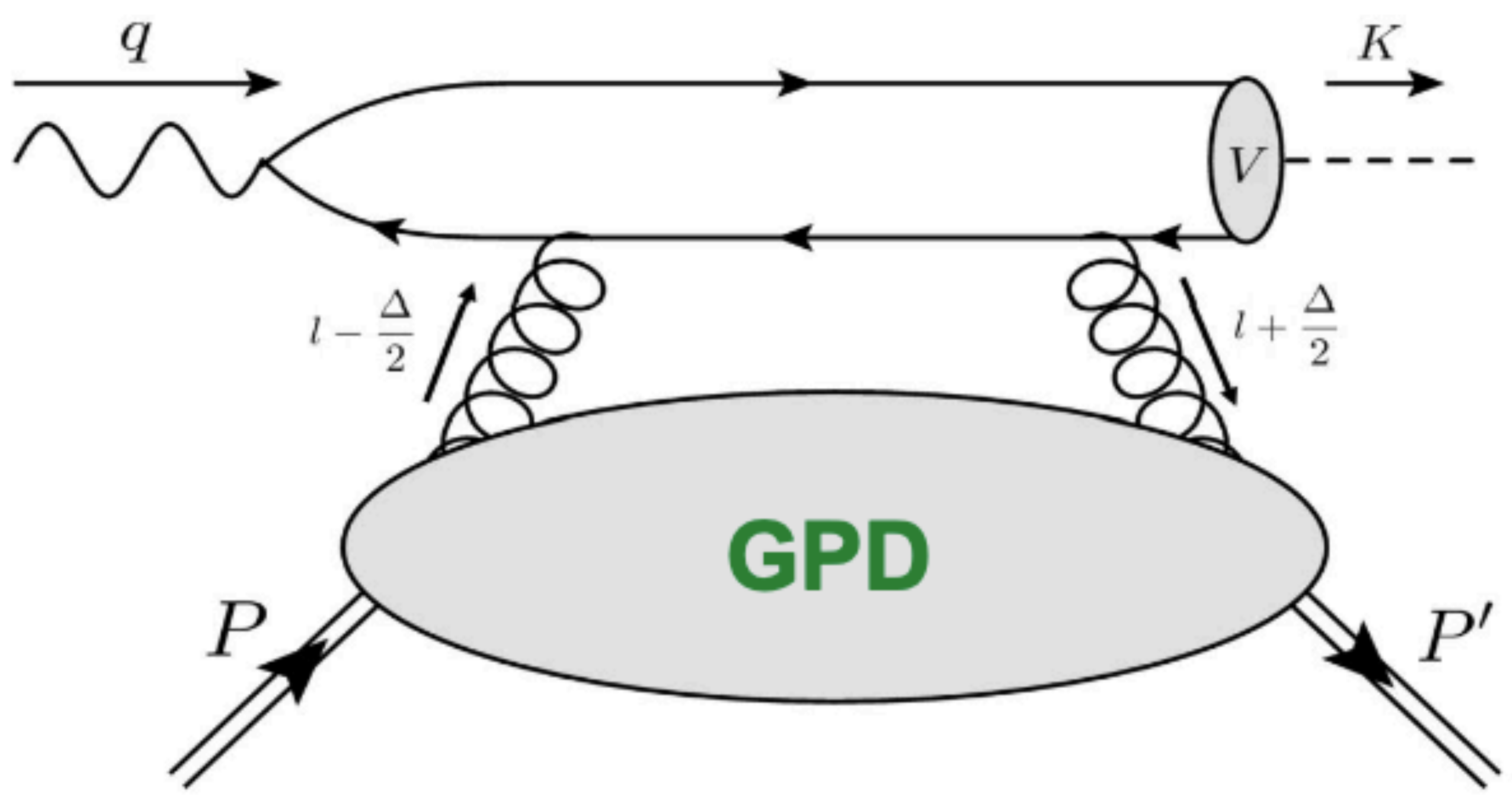

Holography circumvents need for strict factorization but relies on factorization in the Regge sense (at small t)

Hatta & Yang [PRD 98 (2018)074003]
Mamo & Zahed [PRD 101 (2020) 086003]
[PRD 106 (2022) 086004]

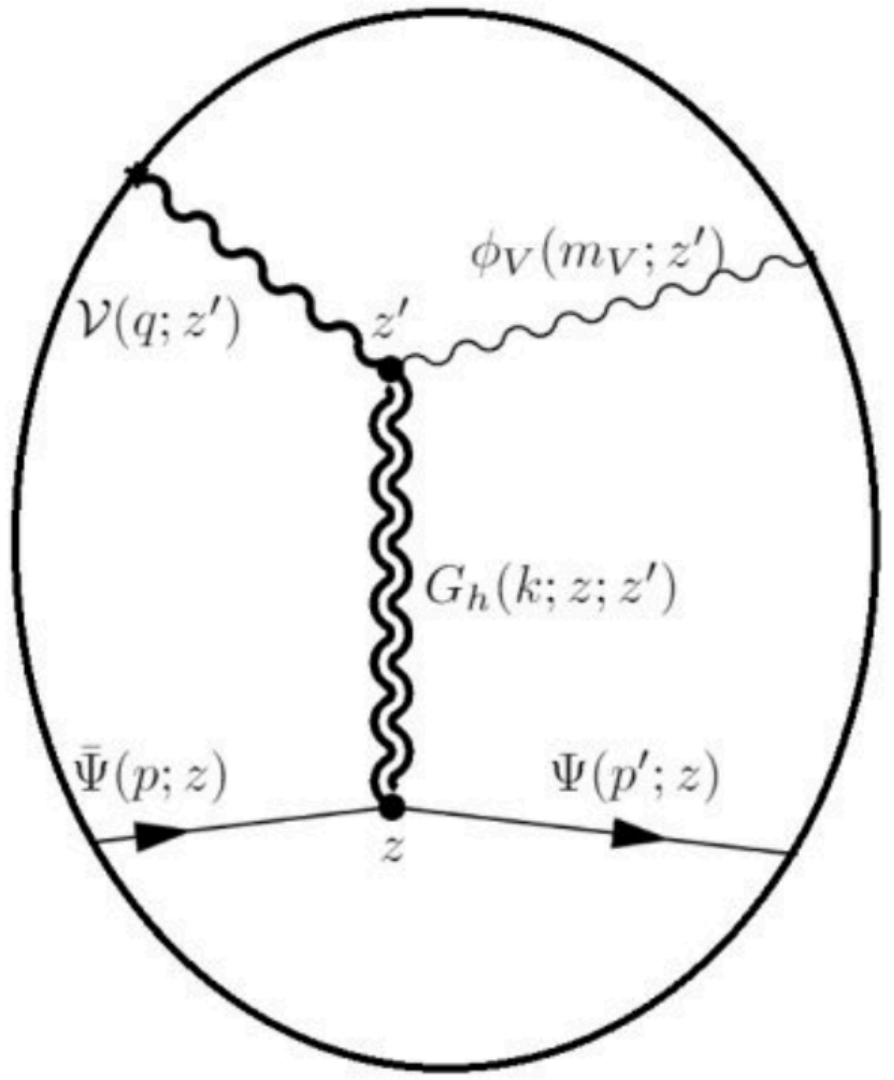

Extraction of proton structure quantities requires "factorization" in the sense of only t-channel exchanges

Strong coupled channels or pentaquark poles break direct connection to the proton structure

Framing the issues

The study of J/ψ photoproduction at low energies has consequences for understanding multiple aspects of nonperturbative QCD:

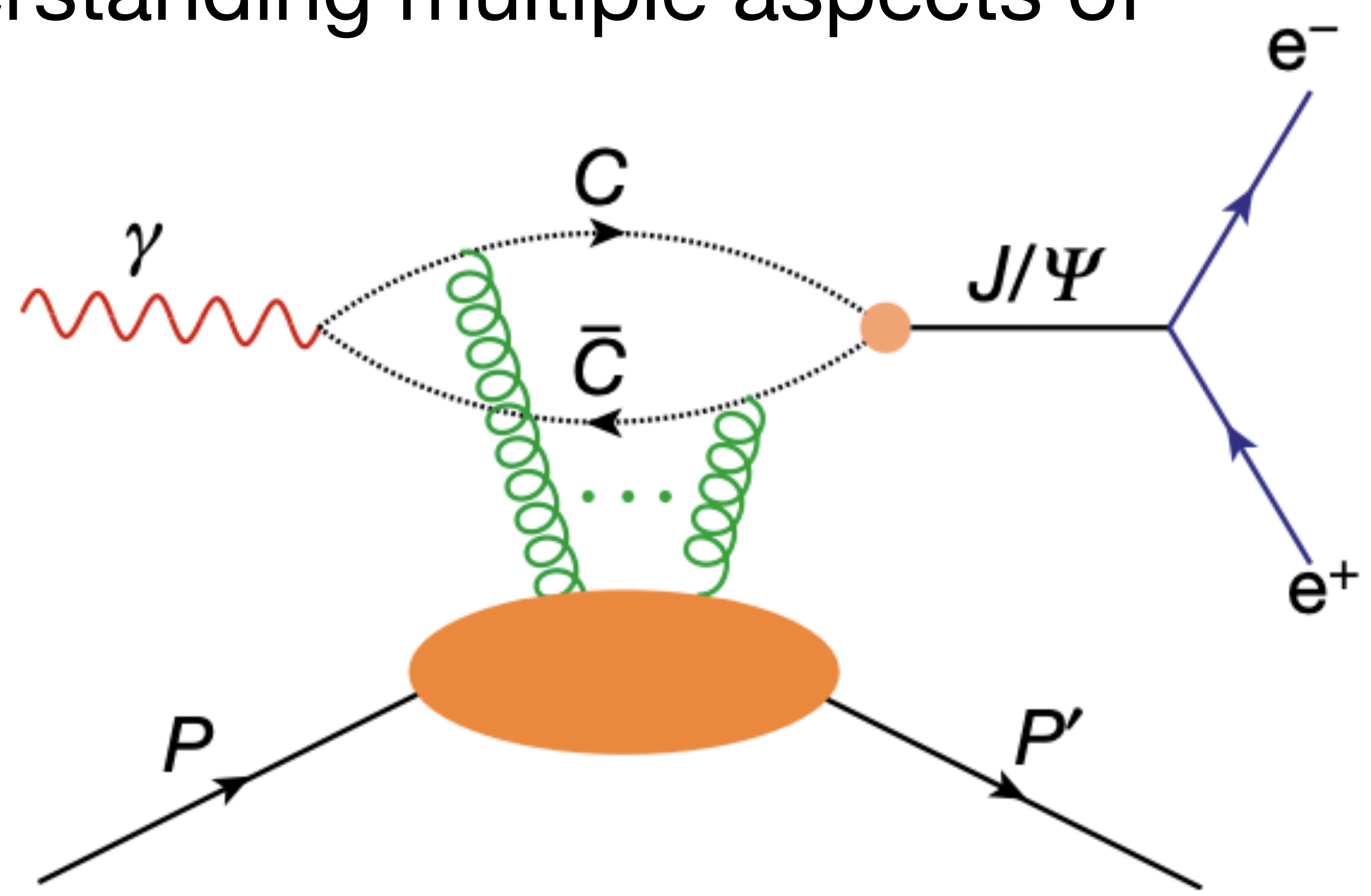

- Mechanical properties of the proton
- Mass radius
- Mass decomposition of the proton (trace anomaly)
- Binding inside nuclei
- Open-charm contributions
- Existence (and determination of properties) of hidden-charm pentaquarks

But…

- Open-charm contributions violate the factorization of the photon-$c\bar{c}$ and nucleon dynamics
- Vector meson dominance is usually employed to extract the physical quantities of interest

Hence:

- **Relevance of the different contributions needs to be assessed based on available experimental information given that future experiments depend on it**
- **We address these questions considering a generic model for the photoproduction amplitude and reliying solely on data**

Jefferson Lab data

GlueX provides integrated cross sections and covers the full kinematic range

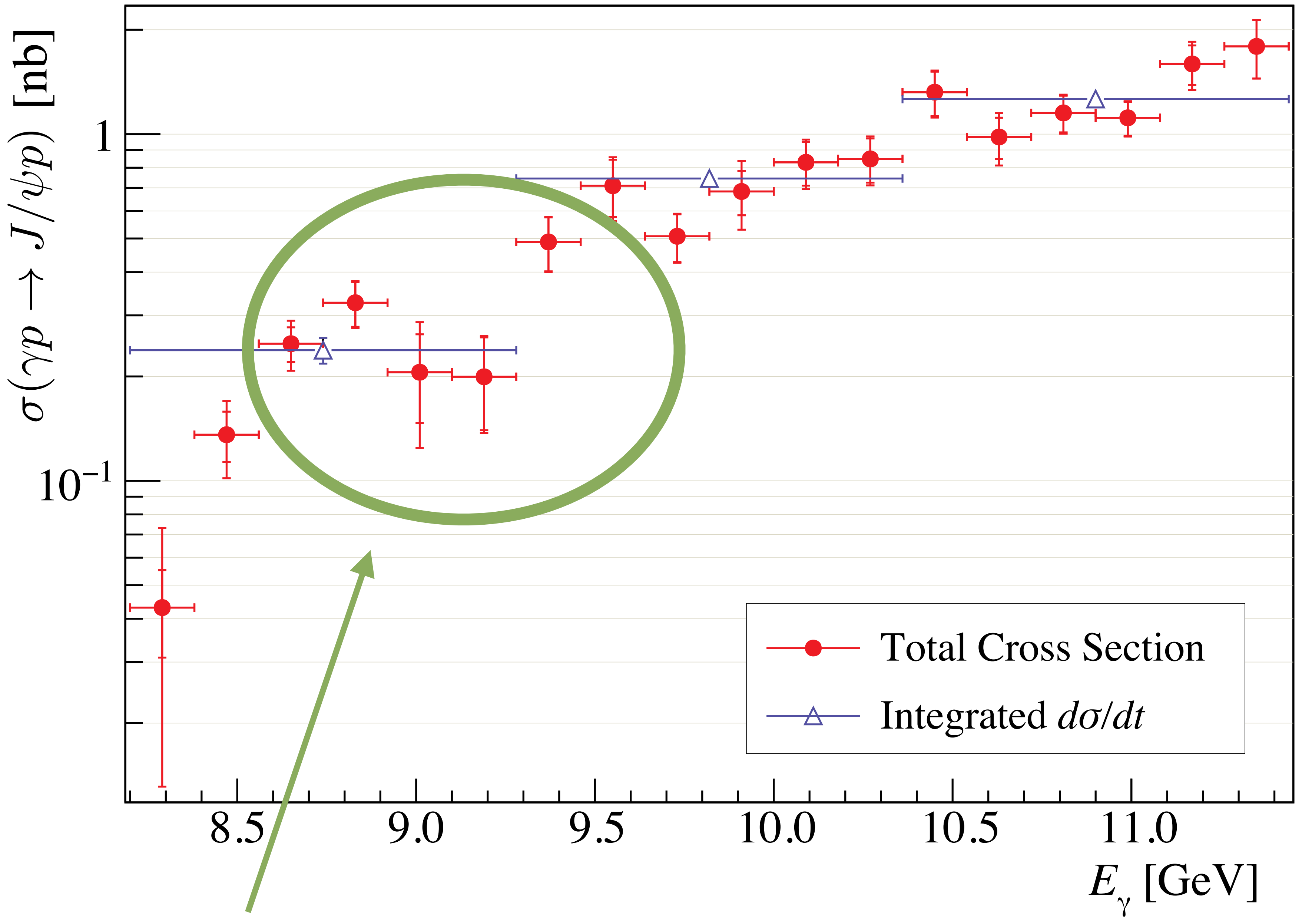

"Dip" established at ~2.6σ compared to a smooth fit

007$^{J/\psi}$

J/ψ-007 [Nature 615 (2023) 813]

GlueX

GlueX [PRC 108 (2023) 025201]

Flattening t-distribution at large momenutm transfer also at ~2.3σ compared to a dipole

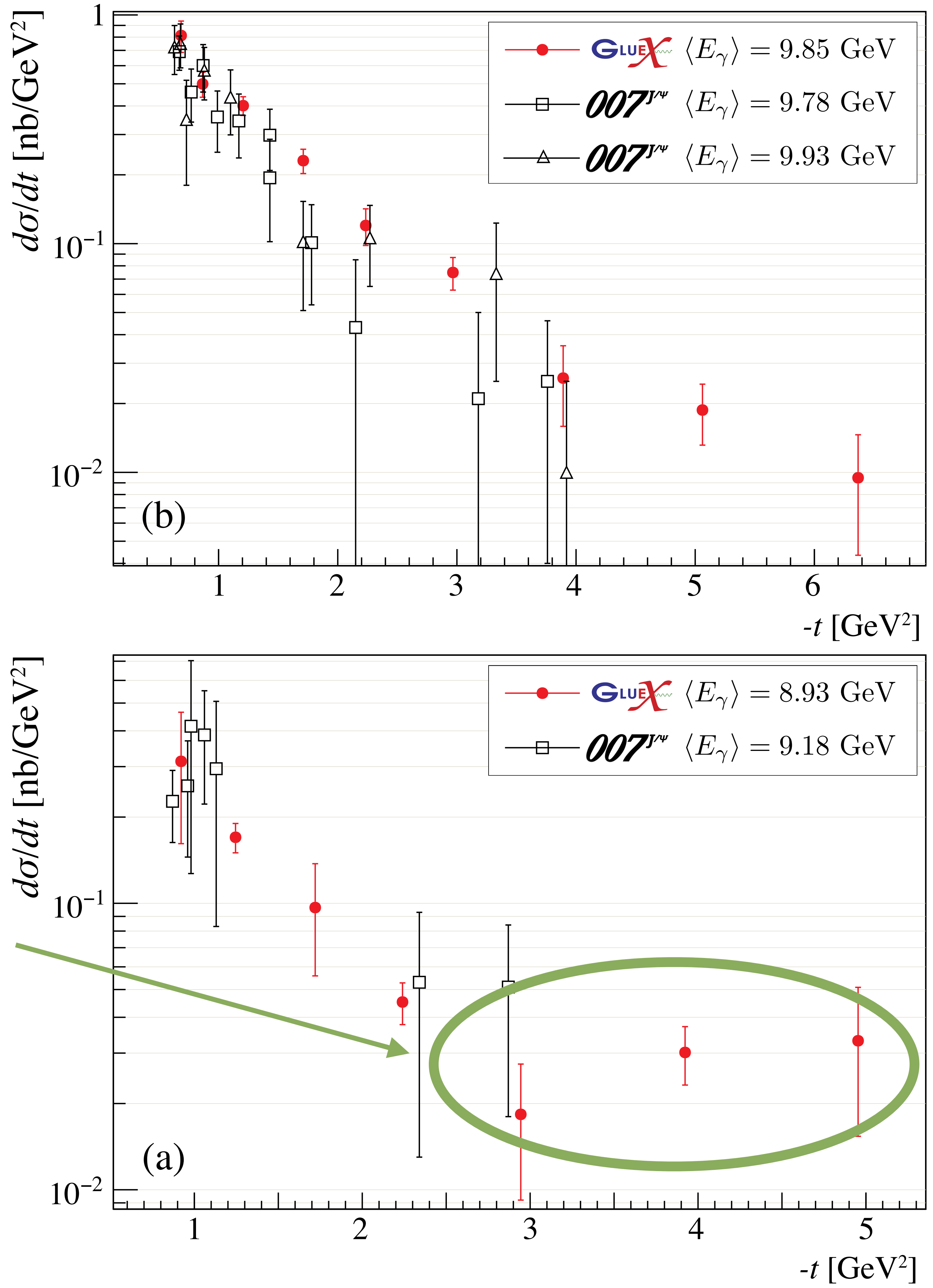

Coupled-channels?
Pentaquarks?

How: P-vector+K-matrix formulation

Winney, et al. (JPAC) [PRD 108 (2023) 054018]
[Zenodo 8302620 (2023)]

Analysis in terms of s-channel partial waves
Ignore spin (no info on asymmetries)

Expansion close to threshold
Finite number of partial waves, consistent with coupled-channels unitarity

$$\frac{d\sigma}{dt} = \frac{1}{16\pi\,(s - m_p^2)^2}\,|\,F(s,t)\,|^2 \qquad F(s,t) = \sum_\ell \left(2\ell + 1\right) P_\ell(\cos\theta_s) F_\ell(s)$$

$$\left.\begin{array}{l} \mathrm{Im}F_\ell = F_\ell \rho T_\ell^\dagger \\ \mathrm{Im}T_\ell = T_\ell \rho T_\ell^\dagger \end{array}\right\} \longrightarrow \quad F_\ell = f_\ell\left(1 + GT_\ell\right) = f_\ell\left(1 - GK_\ell\right)^{-1}$$

where $T_\ell = K_\ell\left(1 - GK_\ell\right)^{-1}$

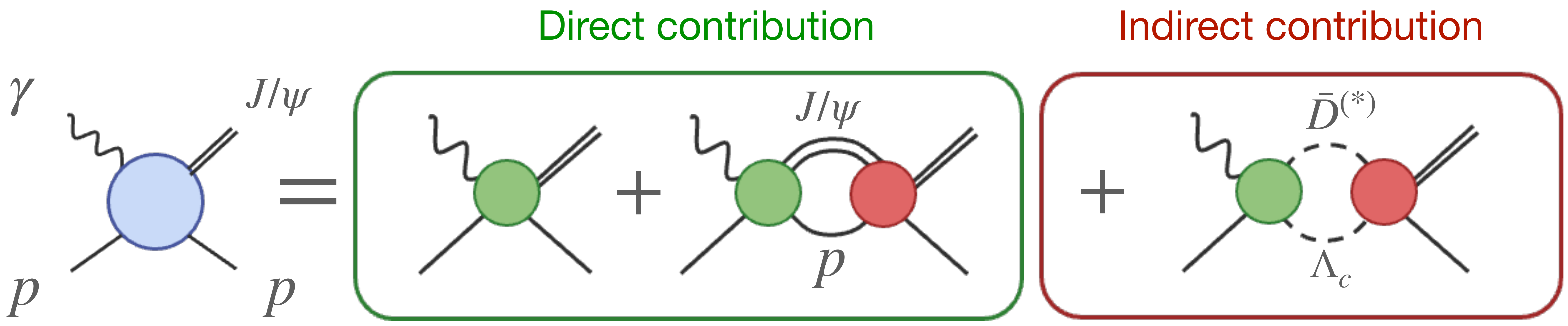

Winney, et al. (JPAC) [PRD 108 (2023) 054018]
[Zenodo 8302620 (2023)]

How: P-vector+K-matrix formulation

$$F_\ell = f_\ell \left(1 - G T_\ell\right)$$

$$T_\ell = \frac{1}{K_\ell^{-1} + G}$$

Advantages:

- Reduced bias
  We do not have model uncertainty from assumed dynamics
  Model is fully analytic and describes the entire kinematical range
  Depends only on the number of terms in the partial wave and near-threshold expansions
  Systematics are testable a posteriori. *L≤3* and effective range work well

- Each partial wave must be parametrized independently
  Production and rescattering only constrained by unitarity

$$f_S = n_S^i \qquad f_\ell = (pq)^\ell n_\ell$$

$$K_S^{ij} = \alpha_S^{ij} + \beta_S^i q_i^2 \delta_{ij} \qquad K_\ell = q^{2\ell}\alpha_\ell$$

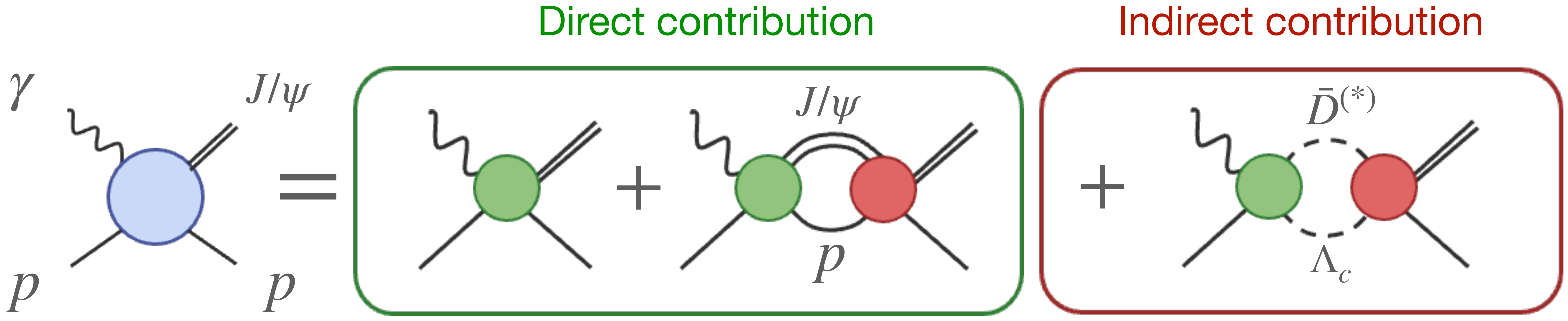

Winney, et al. (JPAC) [PRD 108 (2023) 054018]
[Zenodo 8302620 (2023)]

How: P-vector+K-matrix formulation

We only consider coupled channels in the S wave.

Three models (parametrizations of the S wave):

- <u>Single channel (1C)</u>: Only interactions involving the $J/\psi p$ are included
  Favored by the factorization picture of J/ψ photoproduction
  Base model with respect to which we evaluate the significance of extra thresholds

- <u>Two channels (2C)</u>: We include contributions from an intermediate $\bar{D}^{*}\Lambda_c$ channel

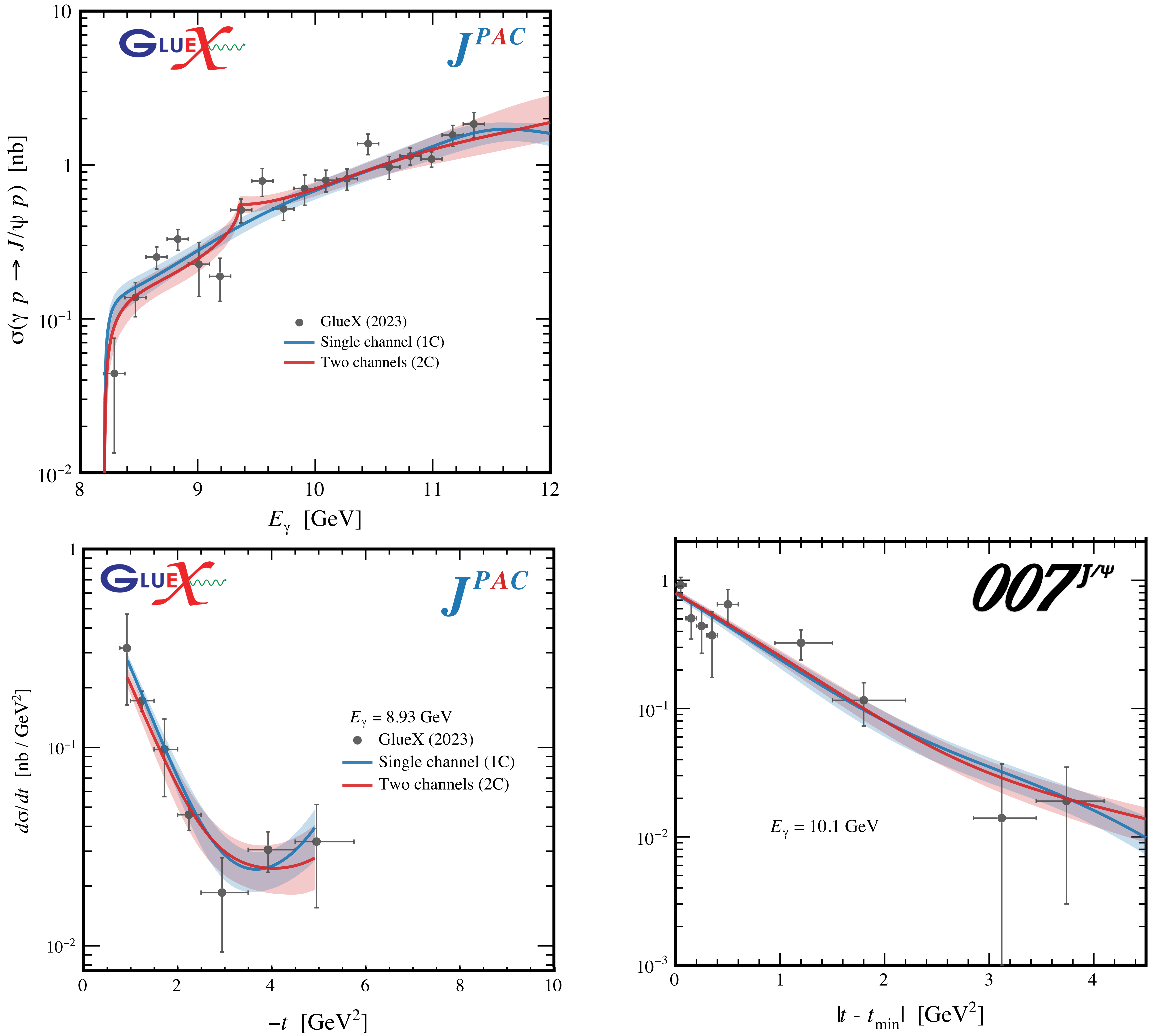

How: P-vector+K-matrix formulation

Winney, et al. (JPAC) [PRD 108 (2023) 054018]
[Zenodo 8302620 (2023)]

We only consider coupled channels in the S wave.

Three models (parametrizations of the S wave):

- Three channels (3C): We include both $\bar{D}^{(*)}\Lambda_c$ channels. We find two classes of solutions We keep only the constant term in the S wave, i.e. $K_S^{ij} = \alpha_S^{ij}$, to have a comparable number of parameters

Even if no explicit K-matrix pole is included, the amplitude can produce poles in the complex energy plane in all three parametrizations $\Longrightarrow$ pentaquarks

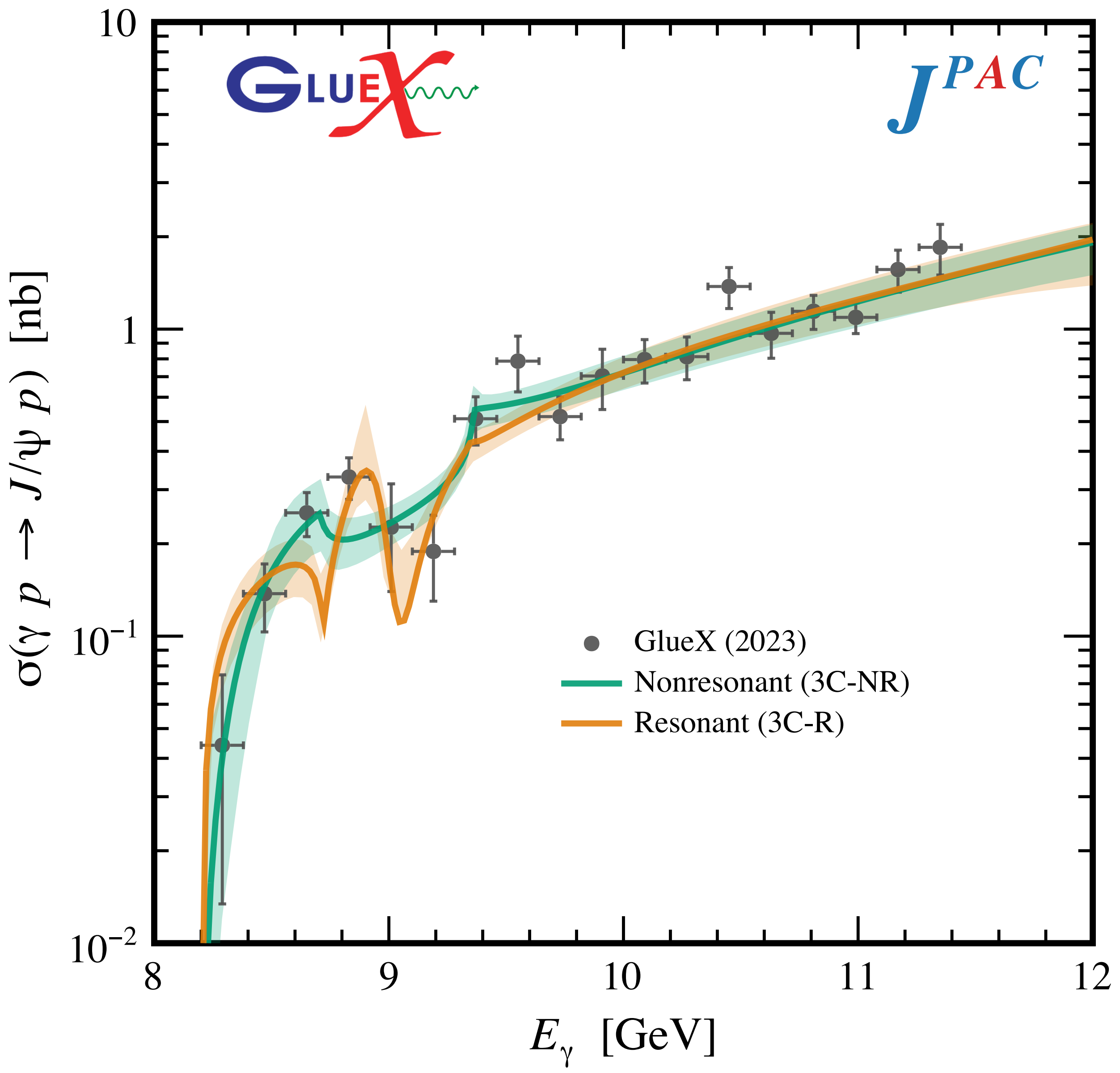

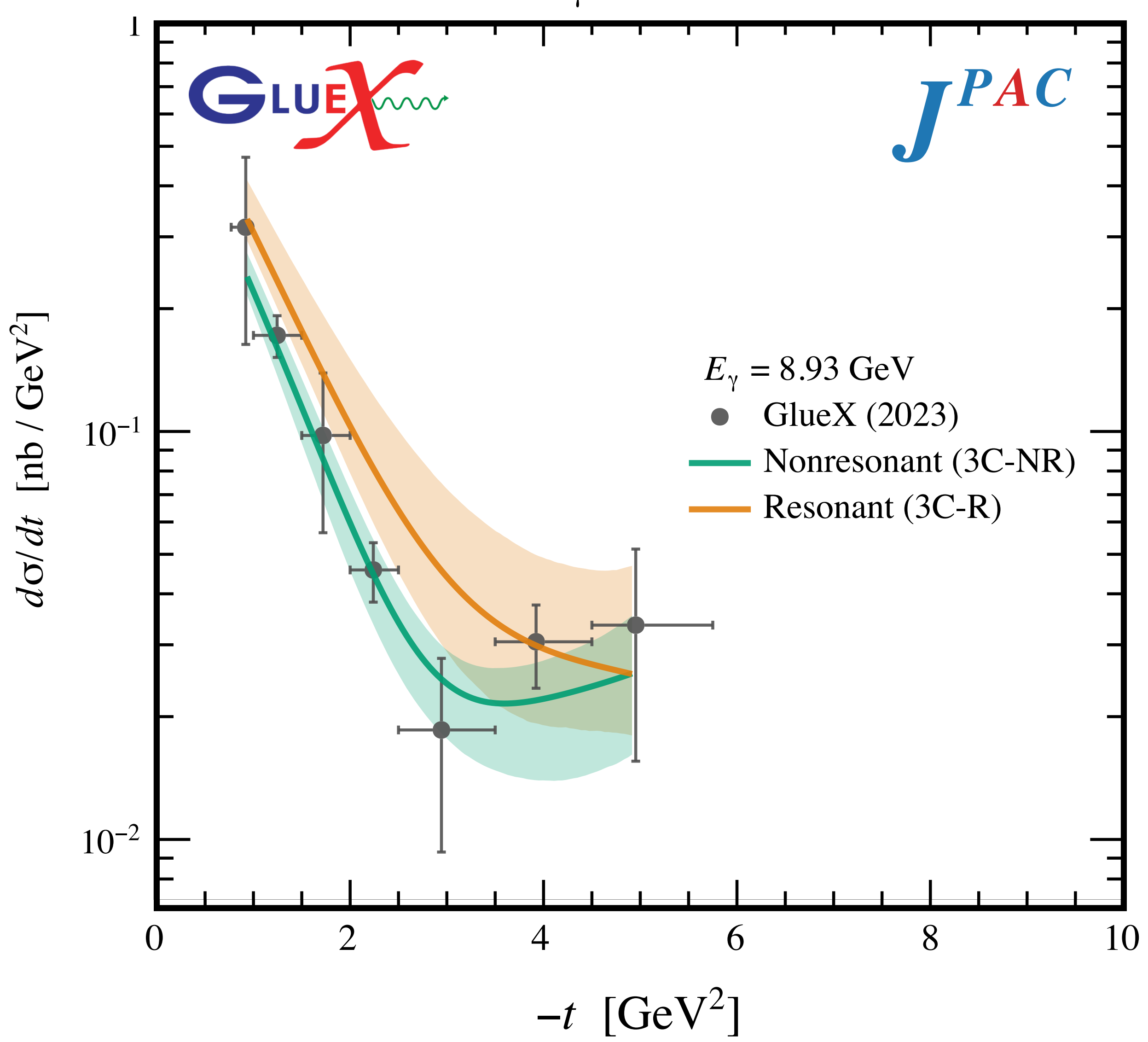

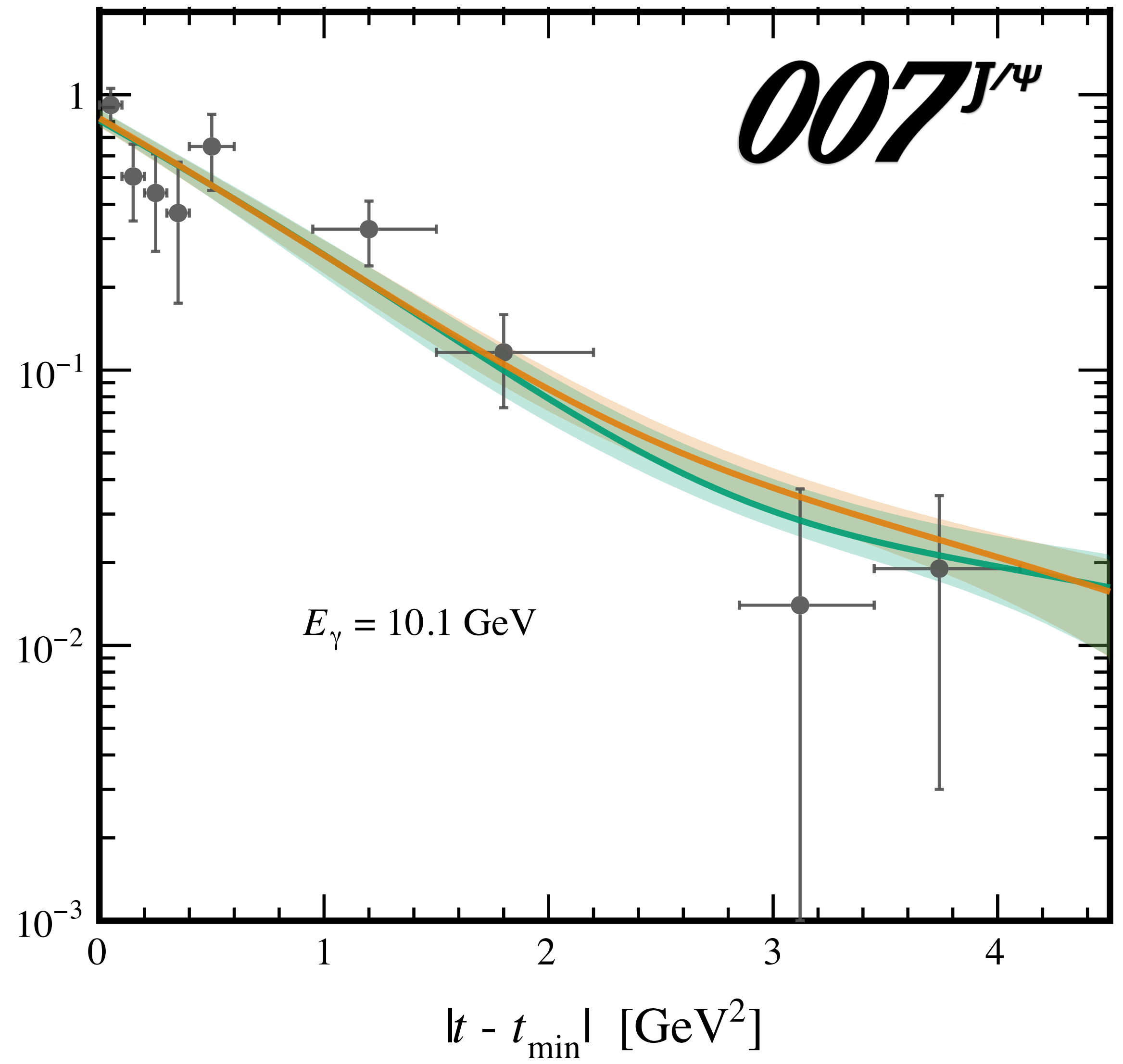

Winney, et al. (JPAC) [PRD 108 (2023) 054018]
[Zenodo 8302620 (2023)]

How: P-vector+K-matrix formulation

We only consider coupled channels in the S wave.

Three models (parametrizations of the S wave):

- Three channels (3C): We include both $\bar{D}^{(*)}\Lambda_c$ channels. We find two classes of solutions We keep only the constant term in the S wave, i.e. $K_S^{ij} = \alpha_S^{ij}$, to have a comparable number of parameters

Even if no explicit K-matrix pole is included, the amplitude can produce poles in the complex energy plane in all three parametrizations $\Longrightarrow$ pentaquarks

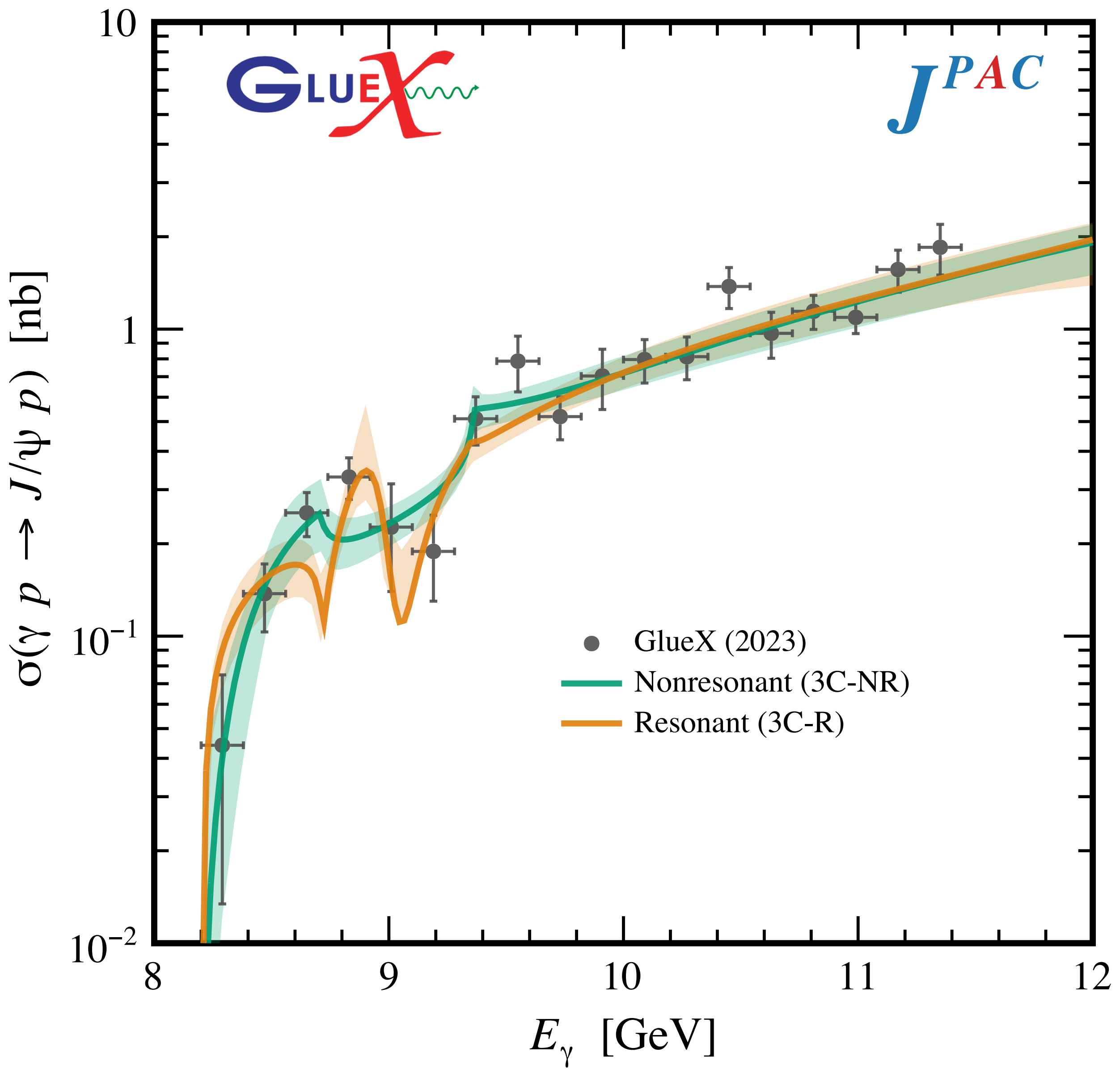

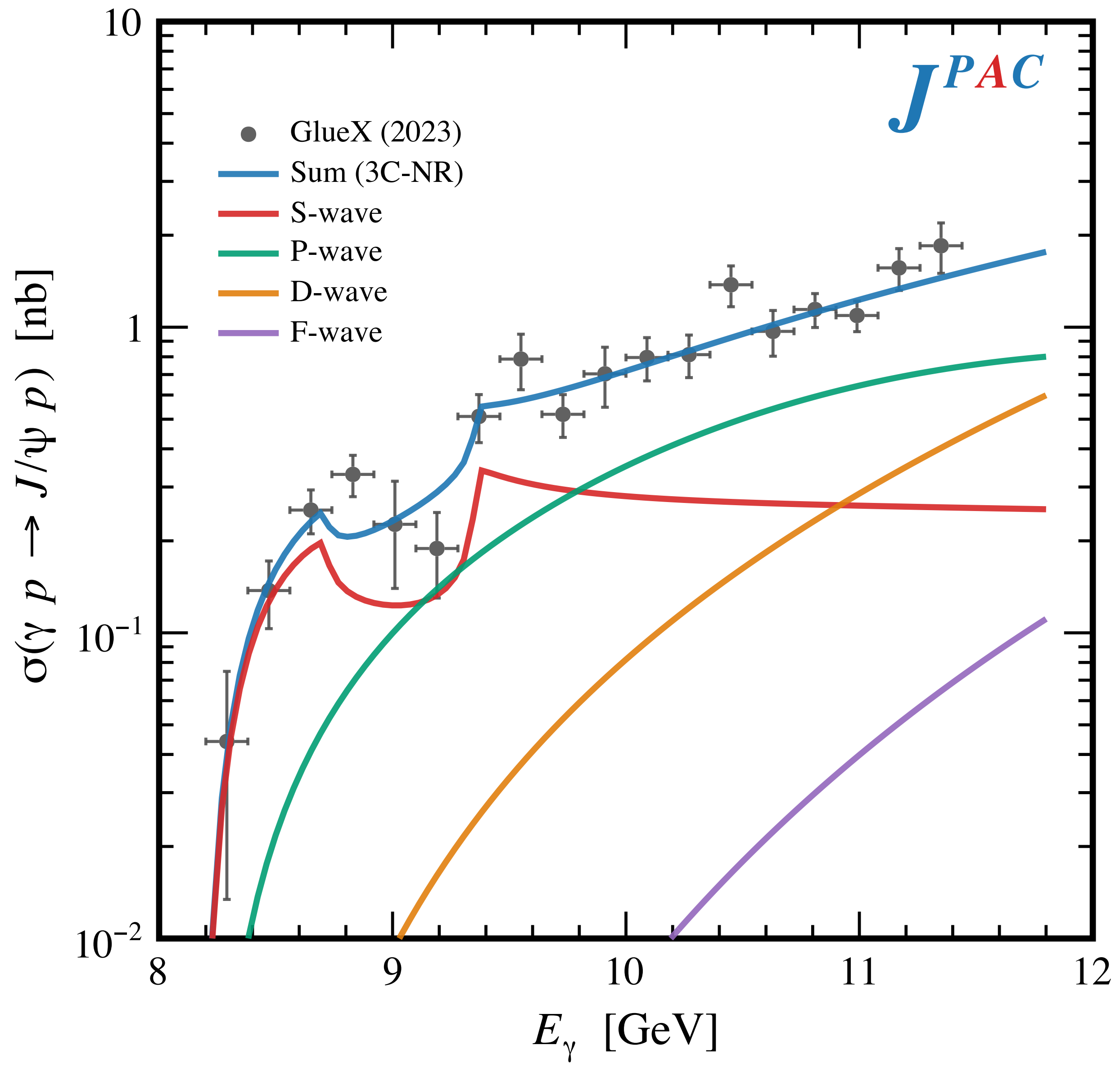

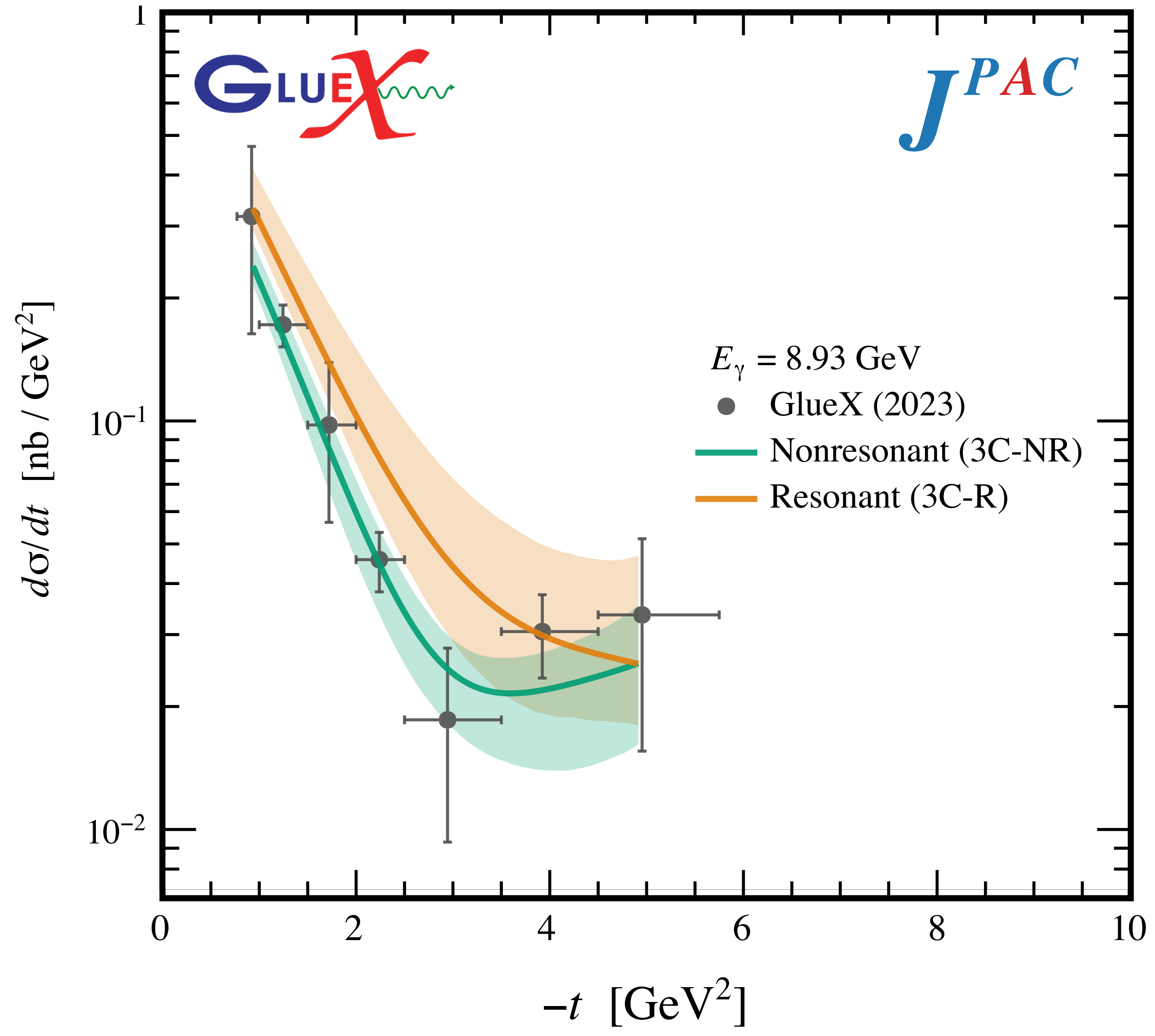

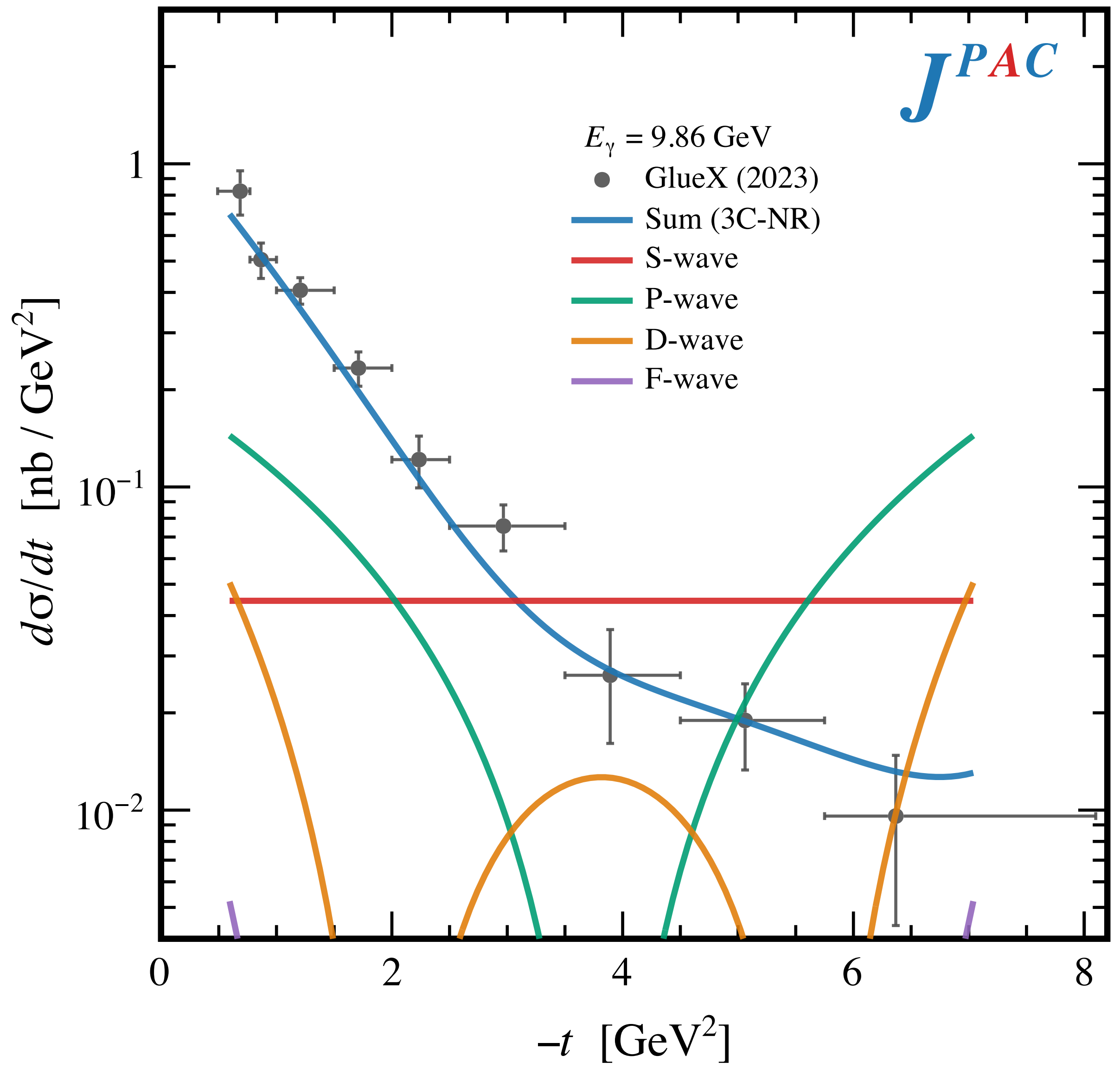

Production mechanisms

Winney, et al. (JPAC) [PRD 108 (2023) 054018]
[Zenodo 8302620 (2023)]

Define the ratio J/ψ of direct photocoupling to all other intermediate channels

Measures the "directness" of the total production at threshold

$$F_S^{\psi p}(s) = \overbrace{n_S^{\psi p}\left(1 + G^{\psi p}\, T_S^{\psi p,\psi p}\right)}^{F^{\psi p}_{\text{direct}}(s)} + \overbrace{\left(n_S^{\bar{D}\Lambda_c}\, G^{\bar{D}\Lambda_c}\, T_S^{\bar{D}\Lambda_c,\psi p} + n_S^{\bar{D}^*\Lambda_c}\, G^{\bar{D}^*\Lambda_c}\, T_S^{\bar{D}^*\Lambda_c,\psi p}\right)}^{F^{\psi p}_{\text{indirect}}(s)}$$

$$\zeta_{\text{th}} = \frac{\left|F^{\psi p}_{\text{direct}}(s_{\text{th}})\right|}{\left|F^{\psi p}_{\text{direct}}(s_{\text{th}})\right| + \left|F^{\psi p}_{\text{indirect}}(s_{\text{th}})\right|}$$

90% CL

1C	1
2C	[0.56, 0.74]
3C-NR	[0.36, 0.63]
3C-R	[0.03, 0.62]

When included, "factorization violating" contributions make up >25% at 90% CL

Direct contribution

Indirect contribution

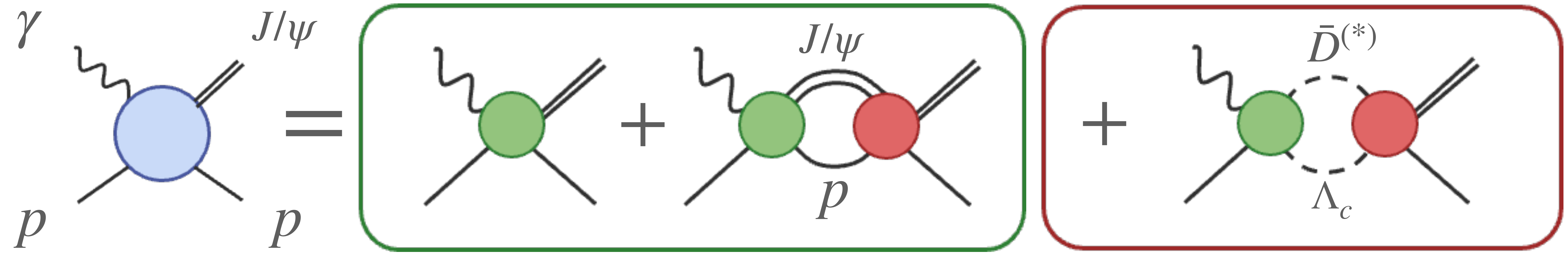

Production mechanisms

Winney, et al. (JPAC) [PRD 108 (2023) 054018]
[Zenodo 8302620 (2023)]

Presence of cusps may indicate large contributions from open charm channels
Complicates the connection to proton structure quantities

90% CL

1C	1
2C	[0.56, 0.74]
3C-NR	[0.36, 0.63]
3C-R	[0.03, 0.62]

Deviations from unity related to the presence of the “dip"

Solution with nearby pentaquark pole consistent with charm exchange dominated production

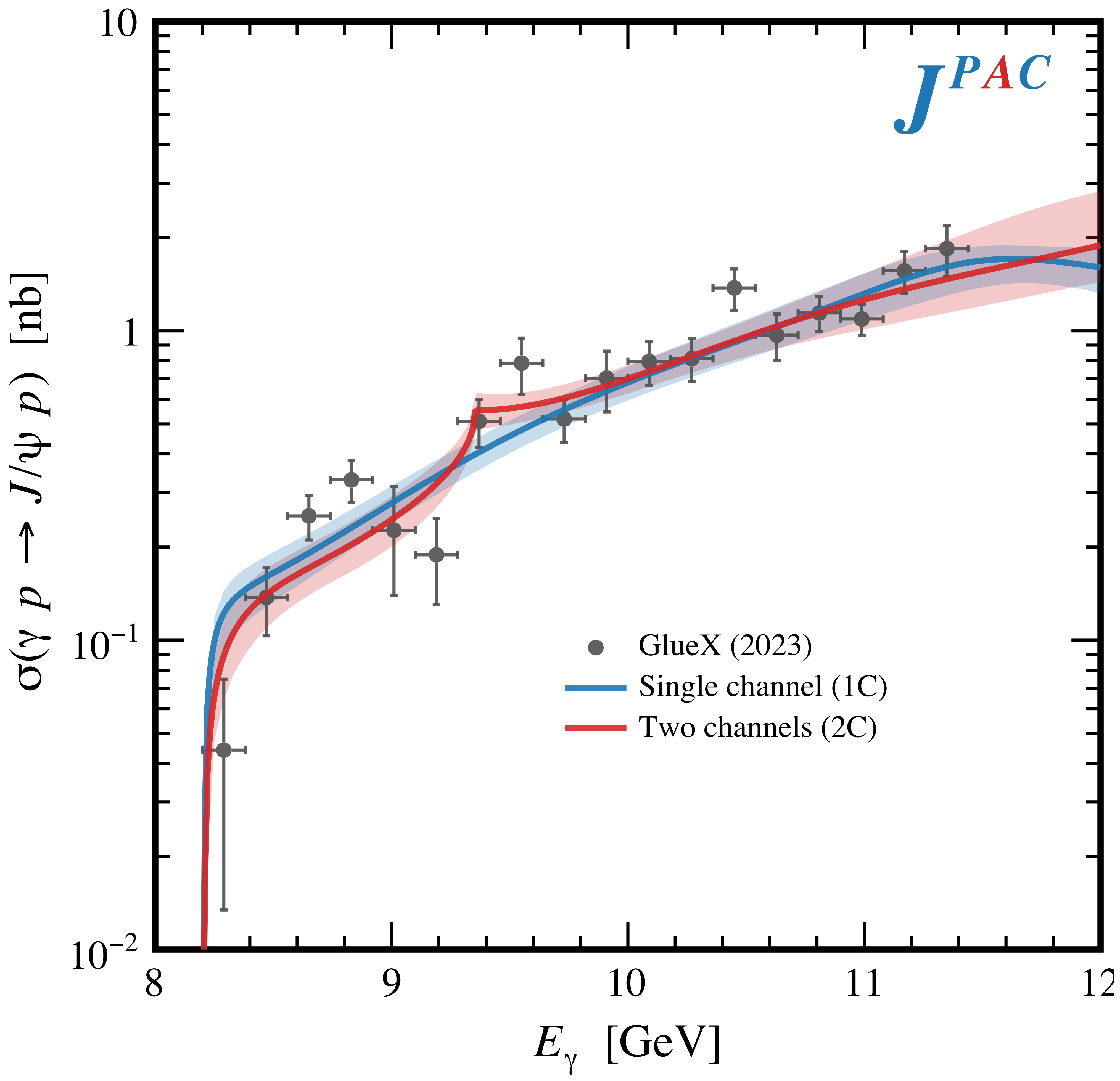

Winney, et al. (JPAC) [PRD 108 (2023) 054018]
[Zenodo 8302620 (2023)]

Pentaquarks

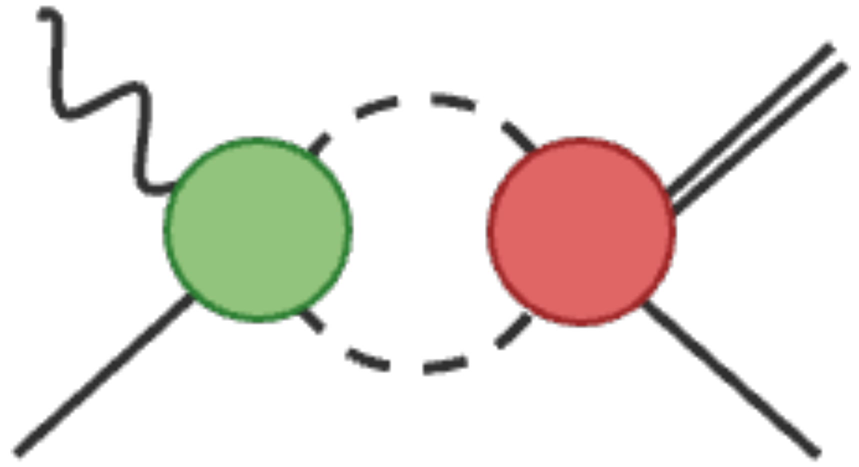

Model is able to generate poles (a.k.a. pentaquarks)
3C-R fit provides a narrow pole on RS=(- - +) in the S wave

$$M = 4211 \text{ MeV} \qquad \Gamma = 48 \text{ MeV}$$

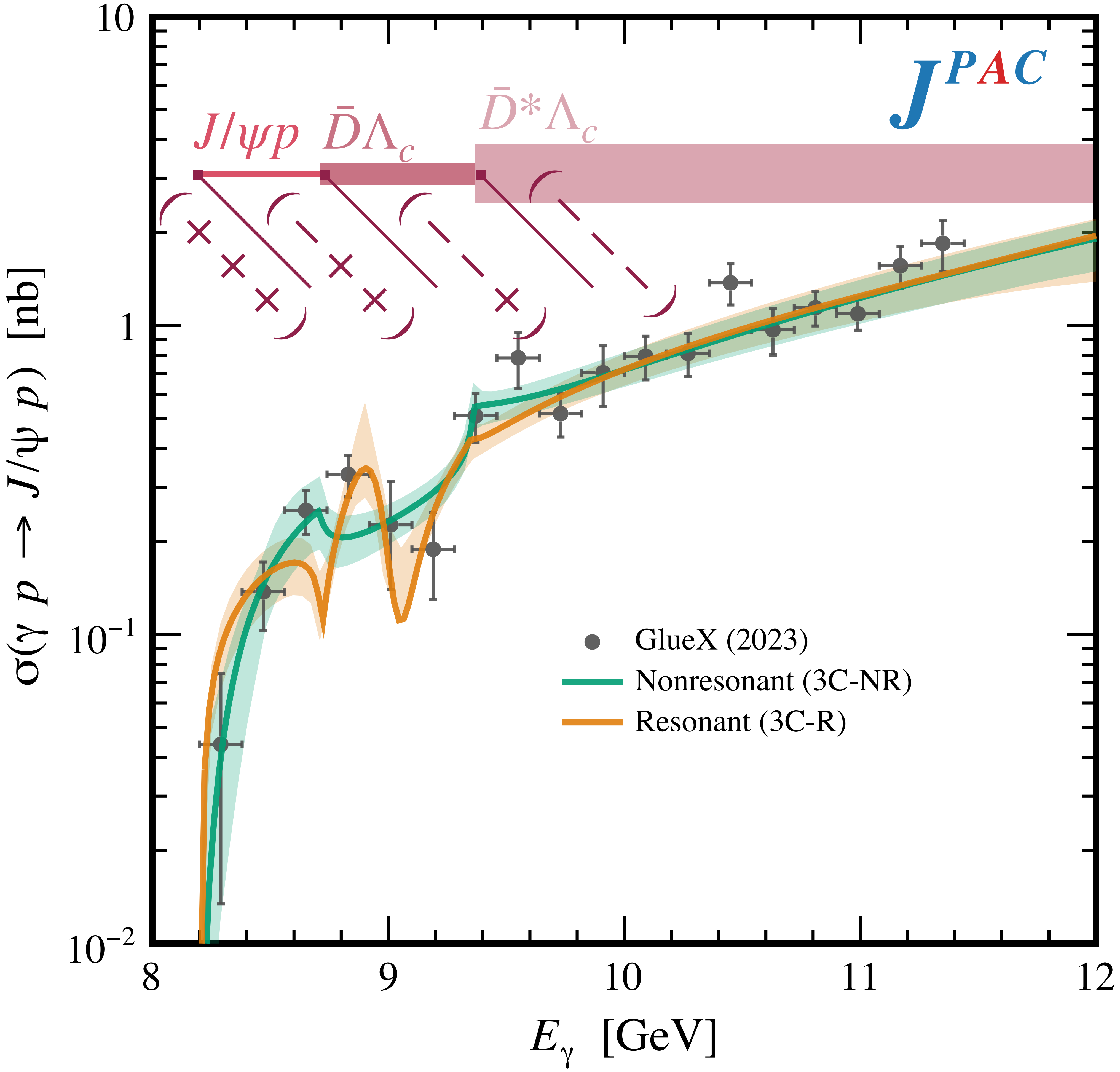

Pole not well constrained
Unable to provide reliable uncertainties

Other poles found on remote Riemann sheets

Pentaquarks

Winney, et al. (JPAC) [PRD 108 (2023) 054018]
[Zenodo 8302620 (2023)]

Model is able to generate poles (a.k.a. pentaquarks)
3C-R fit provides a narrow pole on RS=(- - +) in the S wave

$$M = 4211\ \text{MeV} \qquad \Gamma = 48\ \text{MeV}$$

Pole not well constrained
Unable to provide reliable uncertainties

Other poles found on remote Riemann sheets

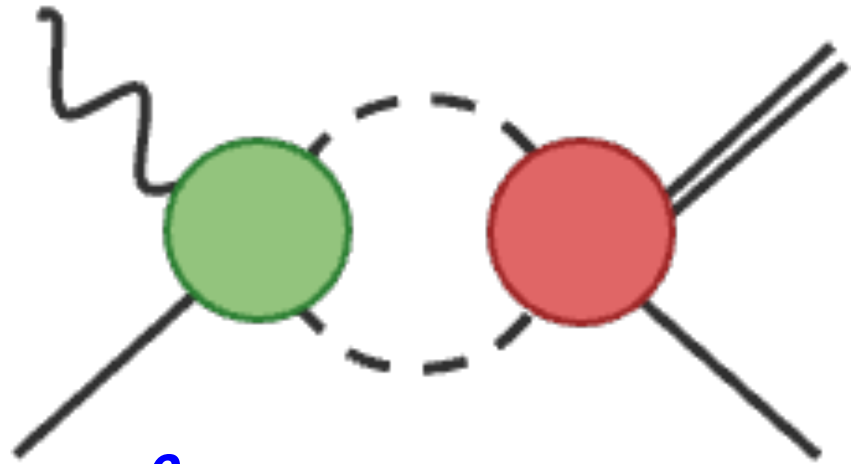

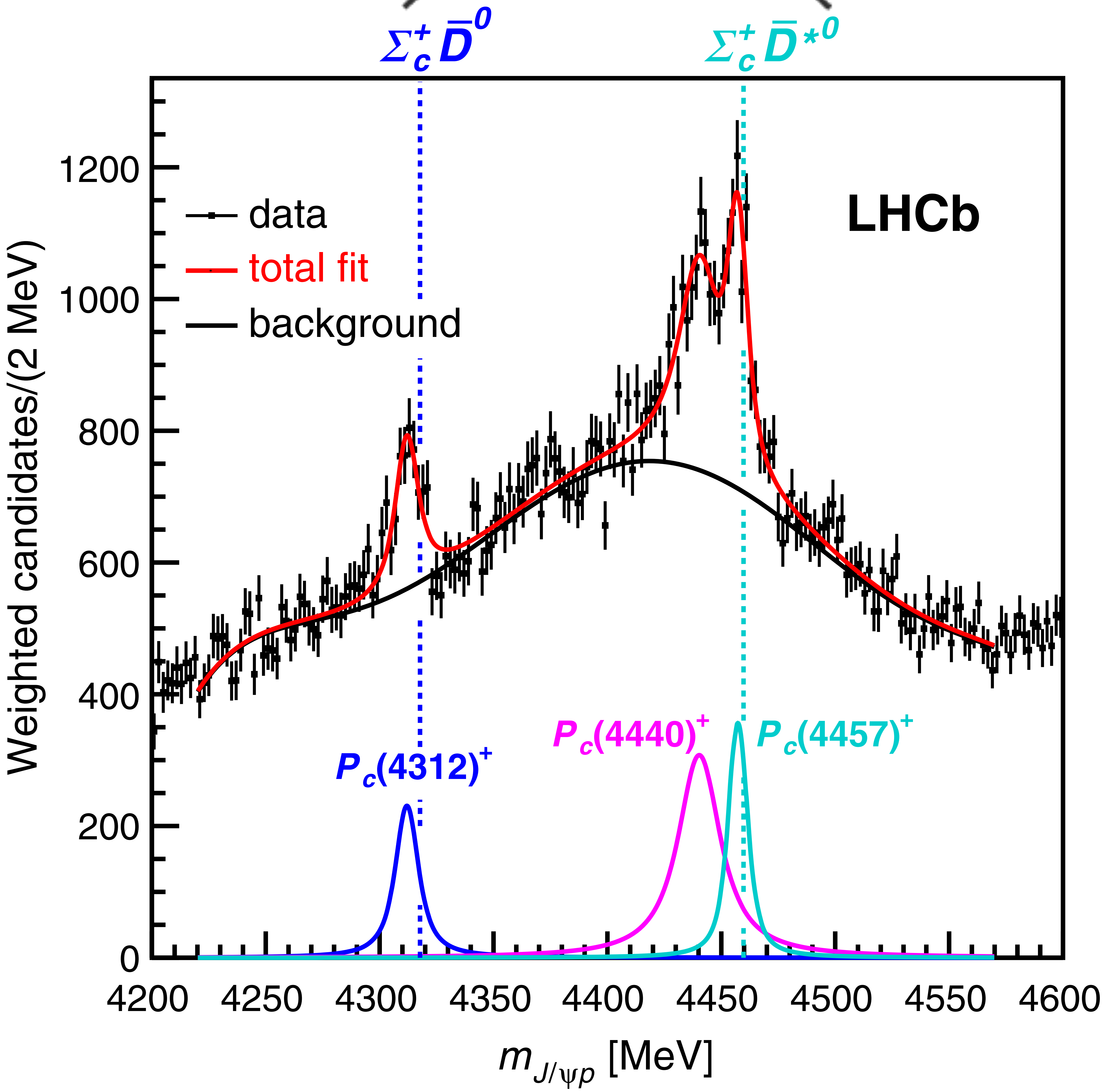

Pentaquarks

Winney, et al. (JPAC) [PRD 108 (2023) 054018]
[Zenodo 8302620 (2023)]

Model is able to generate poles (a.k.a. pentaquarks)
3C-R fit provides a narrow pole on RS=(- - +) in the S wave

$$M = 4211\text{ MeV} \qquad \Gamma = 48\text{ MeV}$$

Pole not well constrained
Unable to provide reliable uncertainties

Other poles found on remote Riemann sheets

We also tested strict VMD and found it to be defficient!!

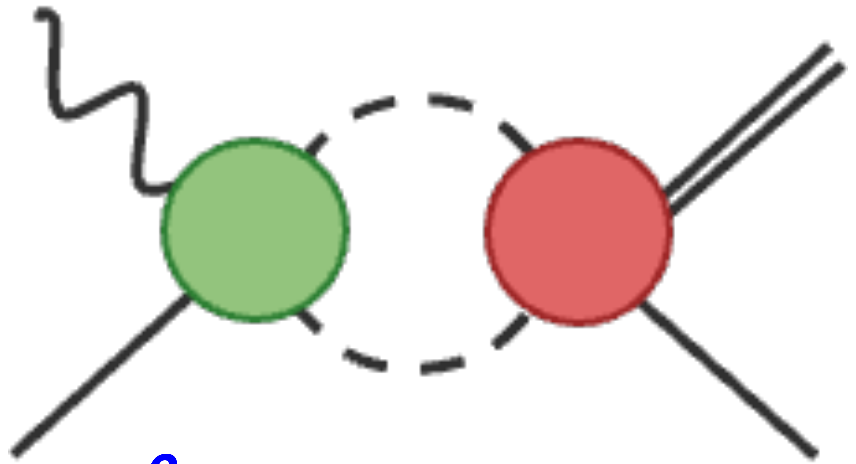

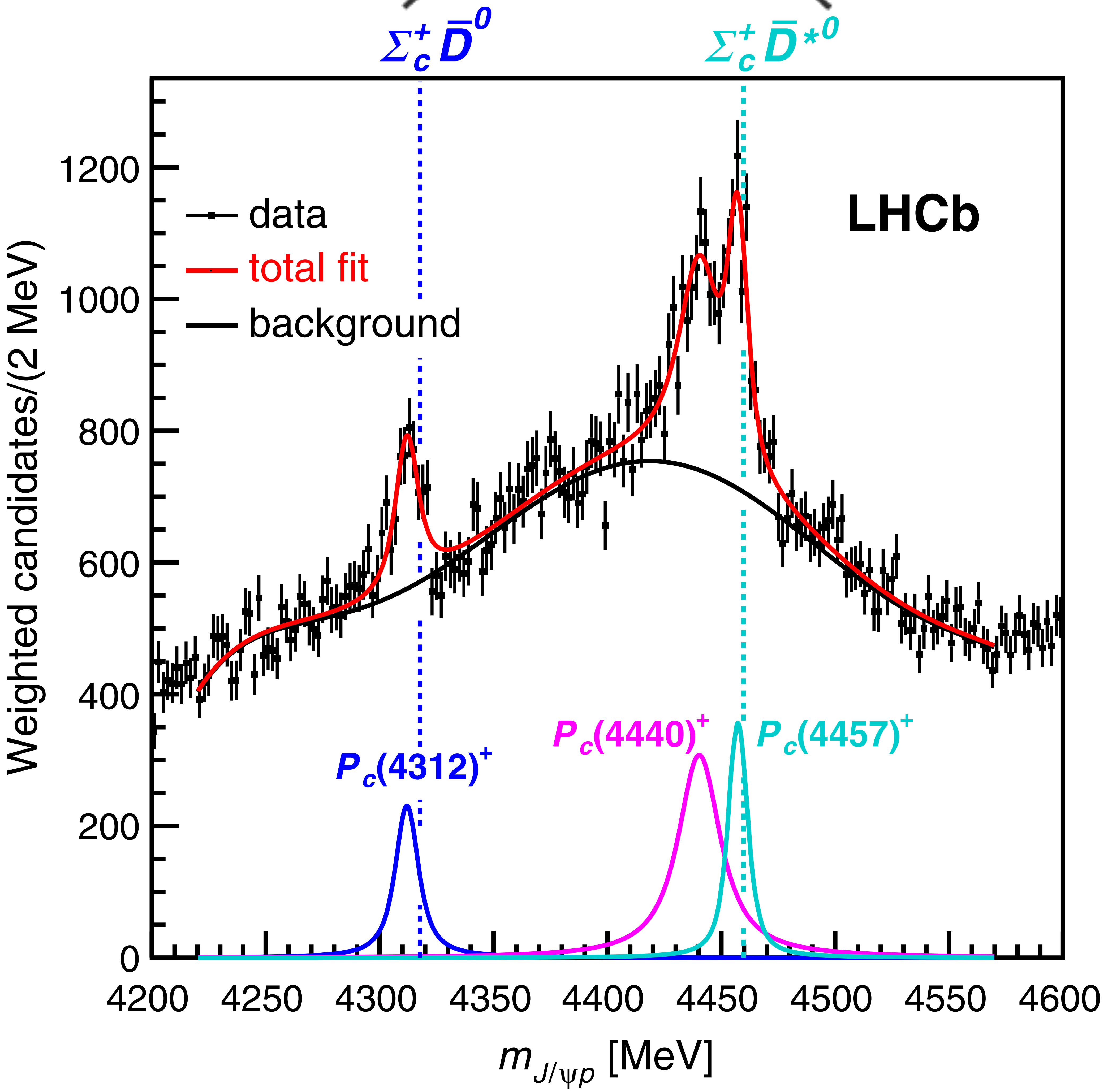

Experimental push at Jefferson Lab

Hall A (SBS) [LOI12-18-001 PAC 46] (SoLID) arXiv:2209.13357
Hall B (CLAS12) [E12-12-001A] (recent publication, on the right)
Hall C [PR12-07-10 PAC 32]
Hall D (GlueX-III) (running, 400/200 days experiment/beam time)

Chatagnon et al. [CLAS 2026]

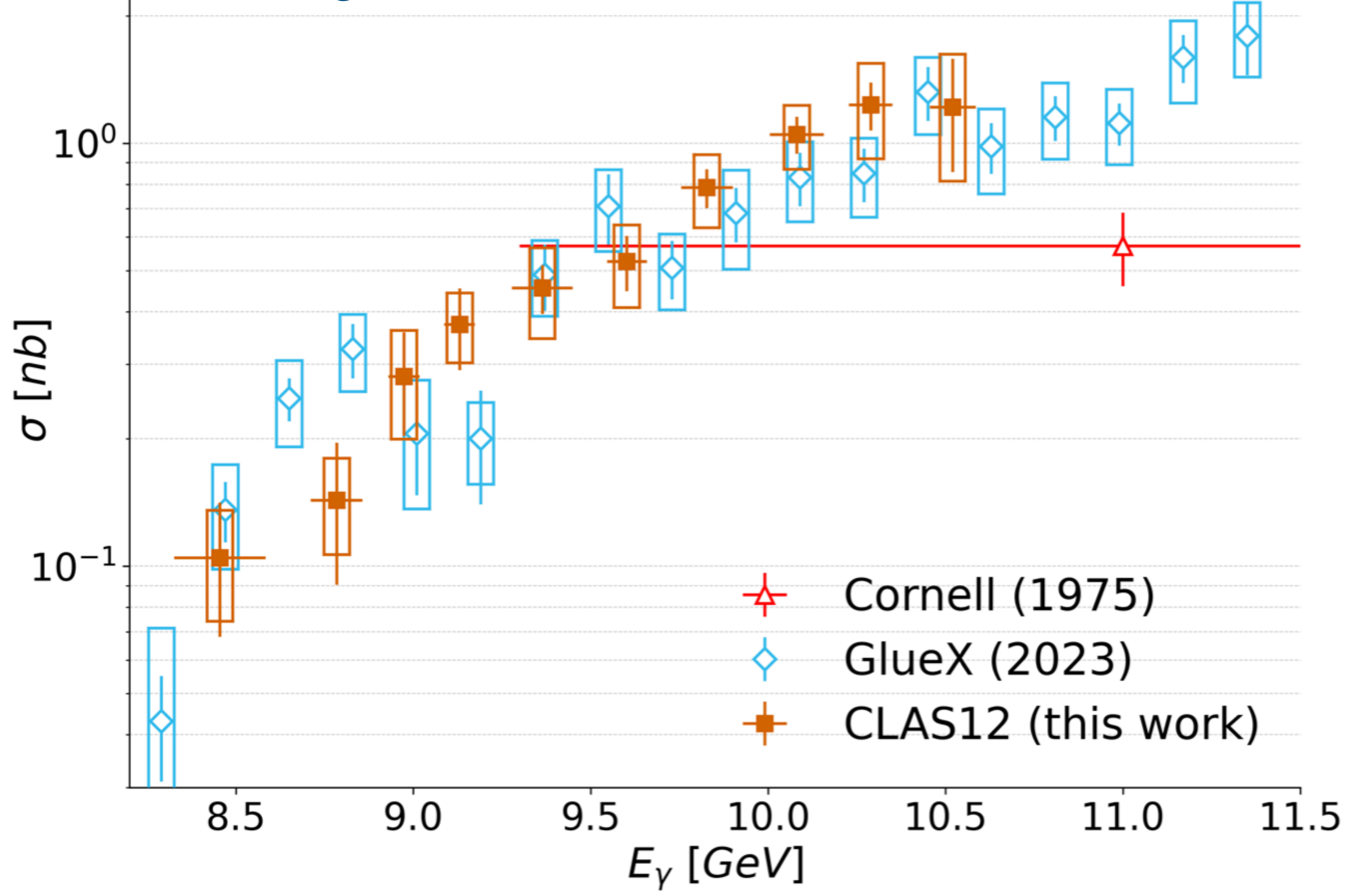

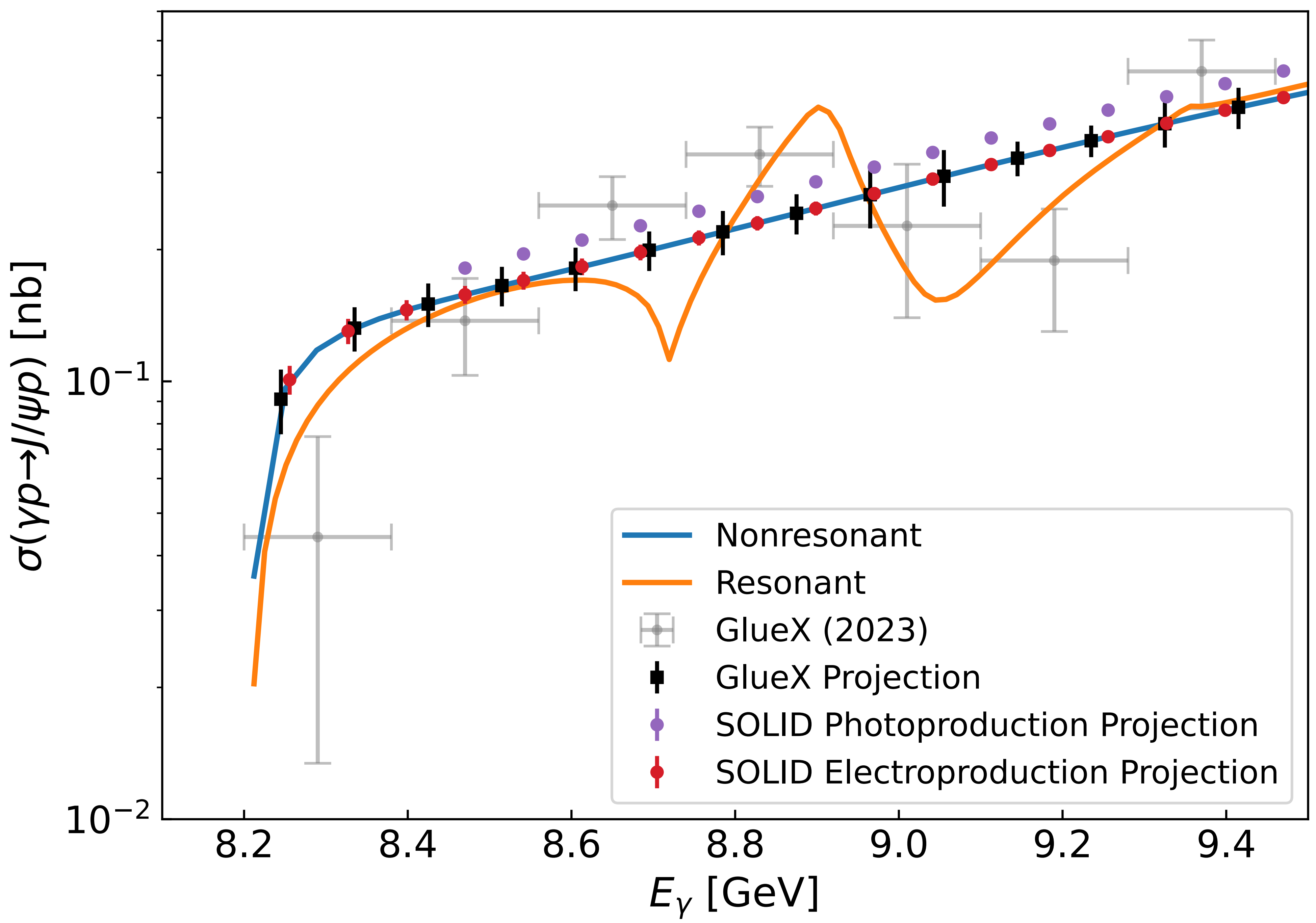

Pentchev & Stevens [Priv. comm. GlueX projection]
Joosten [Priv. comm. SoLID projection]

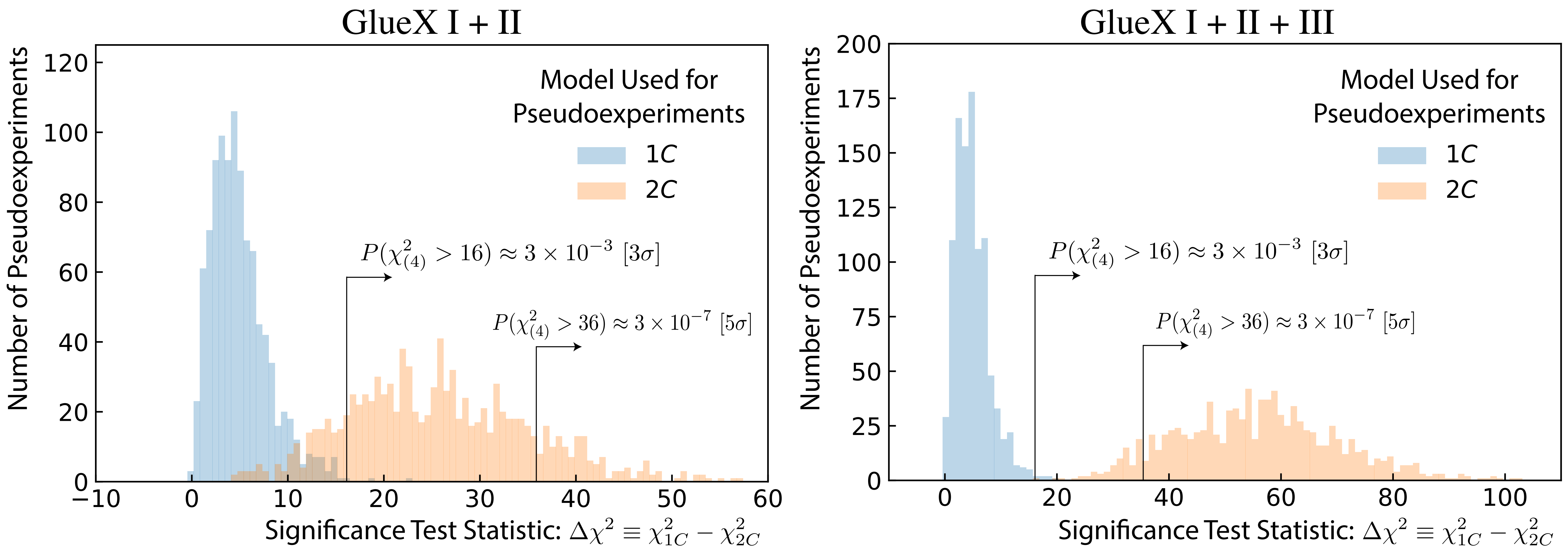

Shepperd et al. [GlueX-III proposal (2024)]

Experimental push at Jefferson Lab

Hall A (SBS) [LOI12-18-001 PAC 46] (SoLID) arXiv:2209.13357
Hall B (CLAS12) [E12-12-001A] (recent publication, on the right)
Hall C [PR12-07-10 PAC 32]
Hall D (GlueX-III) (running, 400/200 days experiment/beam time)

Chatagnon et al. [CLAS 2026]

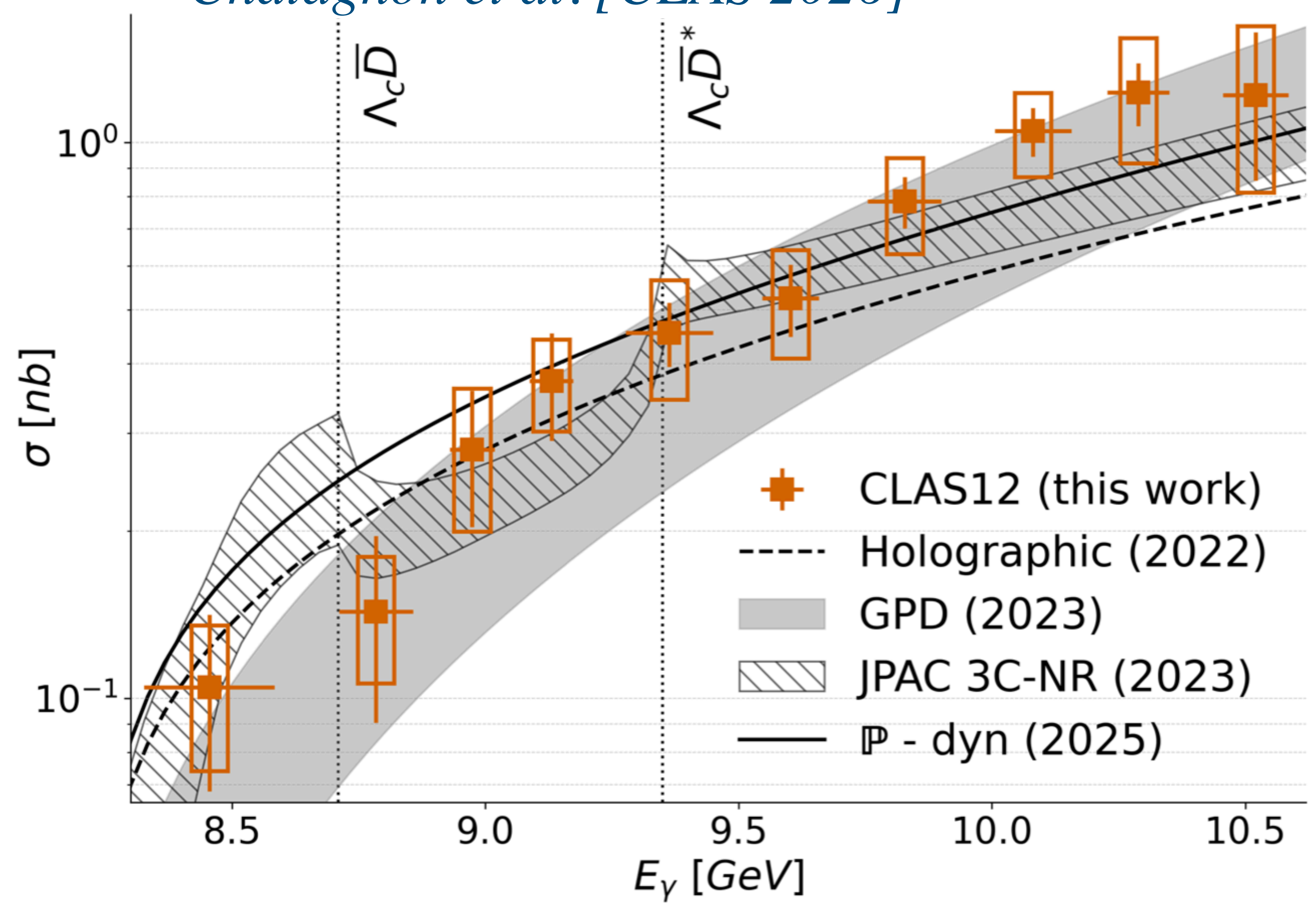

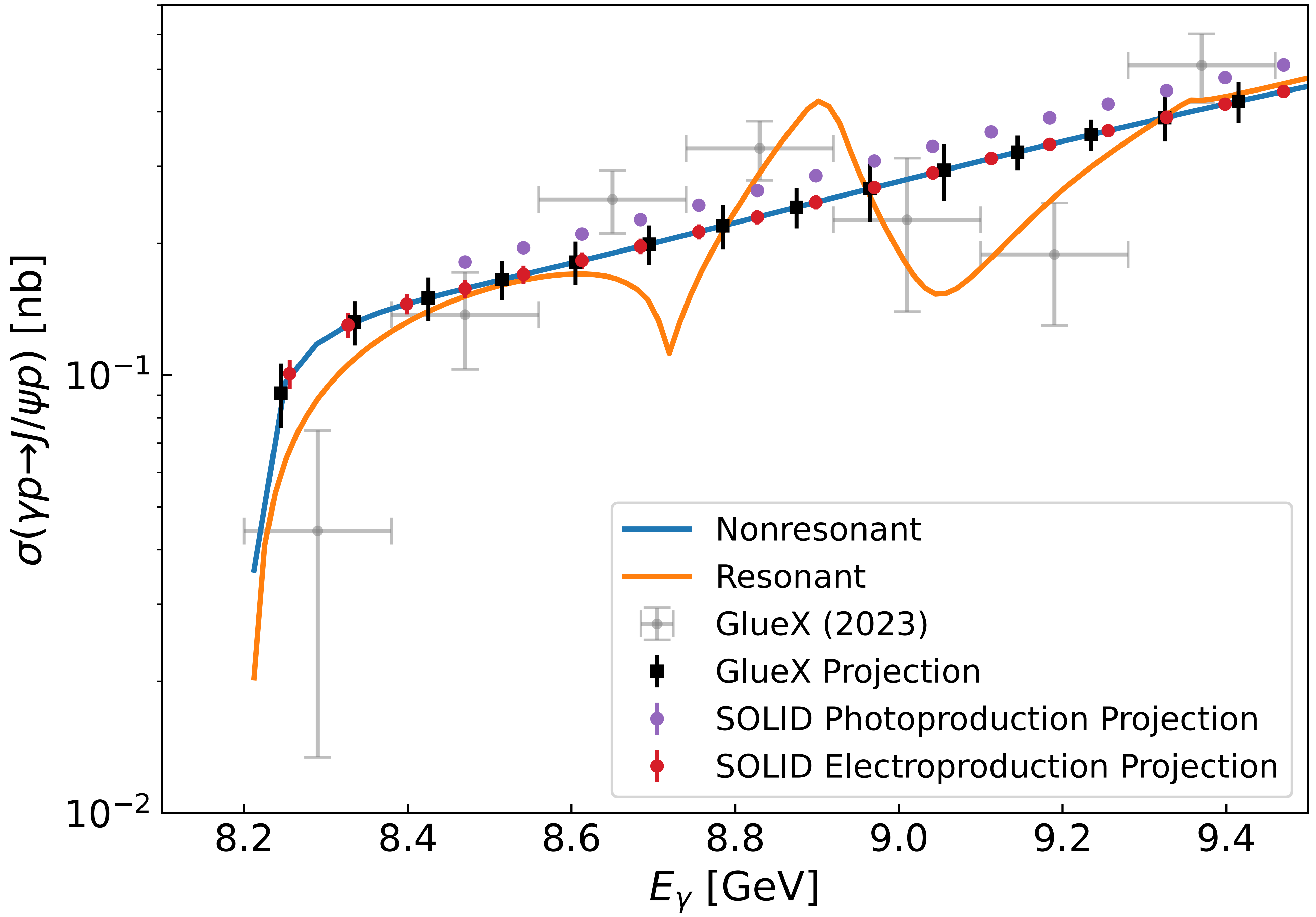

Pentchev & Stevens [Priv. comm. GlueX projection]
Joosten [Priv. comm. SoLID projection]

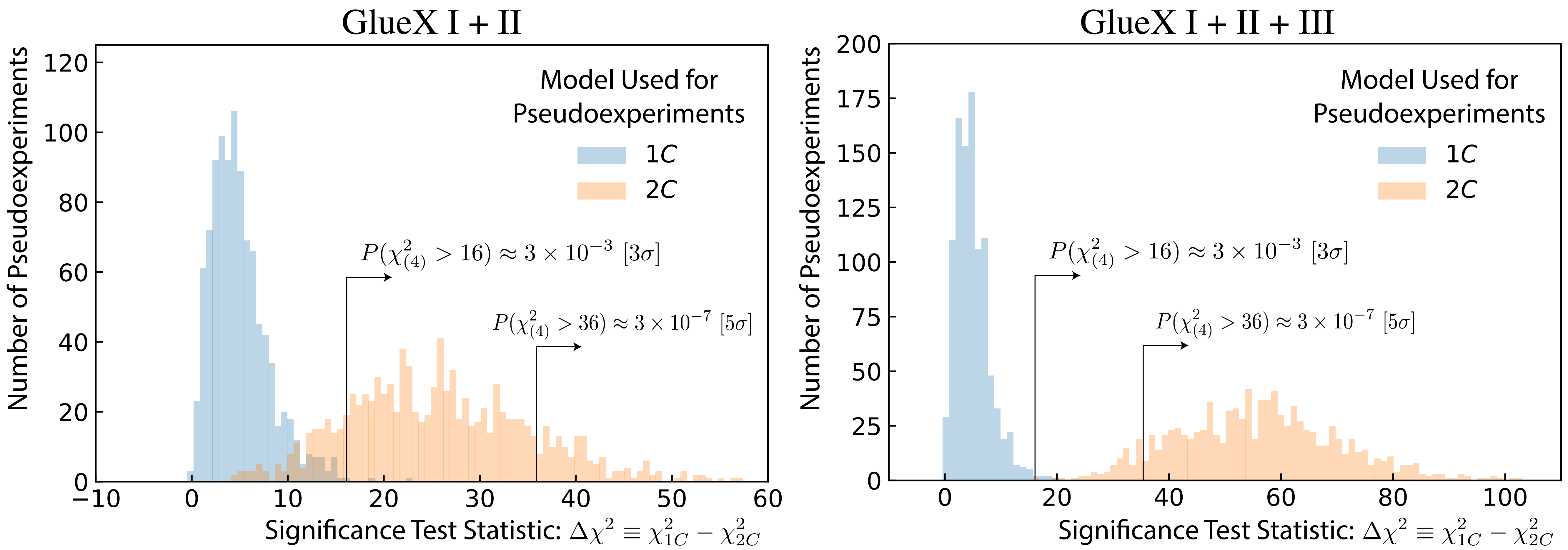

Shepperd et al. [GlueX-III proposal (2024)]

Spin density matrix elements (GlueX/CLAS)

Helicity correlations give key insight on production dynamics (even with unpolarized measurements).

$$\rho^0_{\lambda\lambda'} = \frac{1}{N}\sum_{\lambda_\gamma\lambda_p\lambda_{p'}} \langle\lambda_\gamma,\lambda_p|T|\lambda,\lambda_{p'}\rangle\langle\lambda',\lambda_{p'}|T^*|\lambda_\gamma,\lambda_p\rangle$$

$$\rho^1_{\lambda\lambda'} = \frac{1}{N}\sum_{\lambda_\gamma\lambda_p\lambda_{p'}} \langle\lambda_\gamma,\lambda_p|T|\lambda,\lambda_{p'}\rangle\langle-\lambda',\lambda_{p'}|T^*|\lambda_\gamma,\lambda_p\rangle$$

$$\rho^2_{\lambda\lambda'} = \frac{-i}{N}\sum_{\lambda_\gamma\lambda_p\lambda_{p'}} \lambda_\gamma\langle\lambda_\gamma,\lambda_p|T|\lambda,\lambda_{p'}\rangle\langle-\lambda',\lambda_{p'}|T^*|\lambda_\gamma,\lambda_p\rangle$$

CLAS12 J/ψ polarization needs muon detection!

Factorization often assumes *s*-channel helicity conservation:

$$\langle\lambda_\gamma,\lambda_p|T|\lambda,\lambda_{p'}\rangle \propto (\epsilon_\gamma\cdot\epsilon^*_\psi) \propto \delta_{\lambda_\gamma\lambda_\psi}$$

$$\rho^\alpha_{\lambda,\lambda'} = 0 \quad \text{except} \quad \rho^1_{1,-1} = -\mathrm{Im}\,\rho^2_{1,-1} = \frac{1}{2}$$

Guo et al. [Phys.Rev.D 103 (2021) 9, 096010]

$$\mathcal{M}(\varepsilon_V,\varepsilon) = \frac{8\sqrt{2}\pi\alpha_S(M_V)}{M_V^2}\phi^*(0)G(t,\xi)(\varepsilon^*_V\cdot\varepsilon)$$

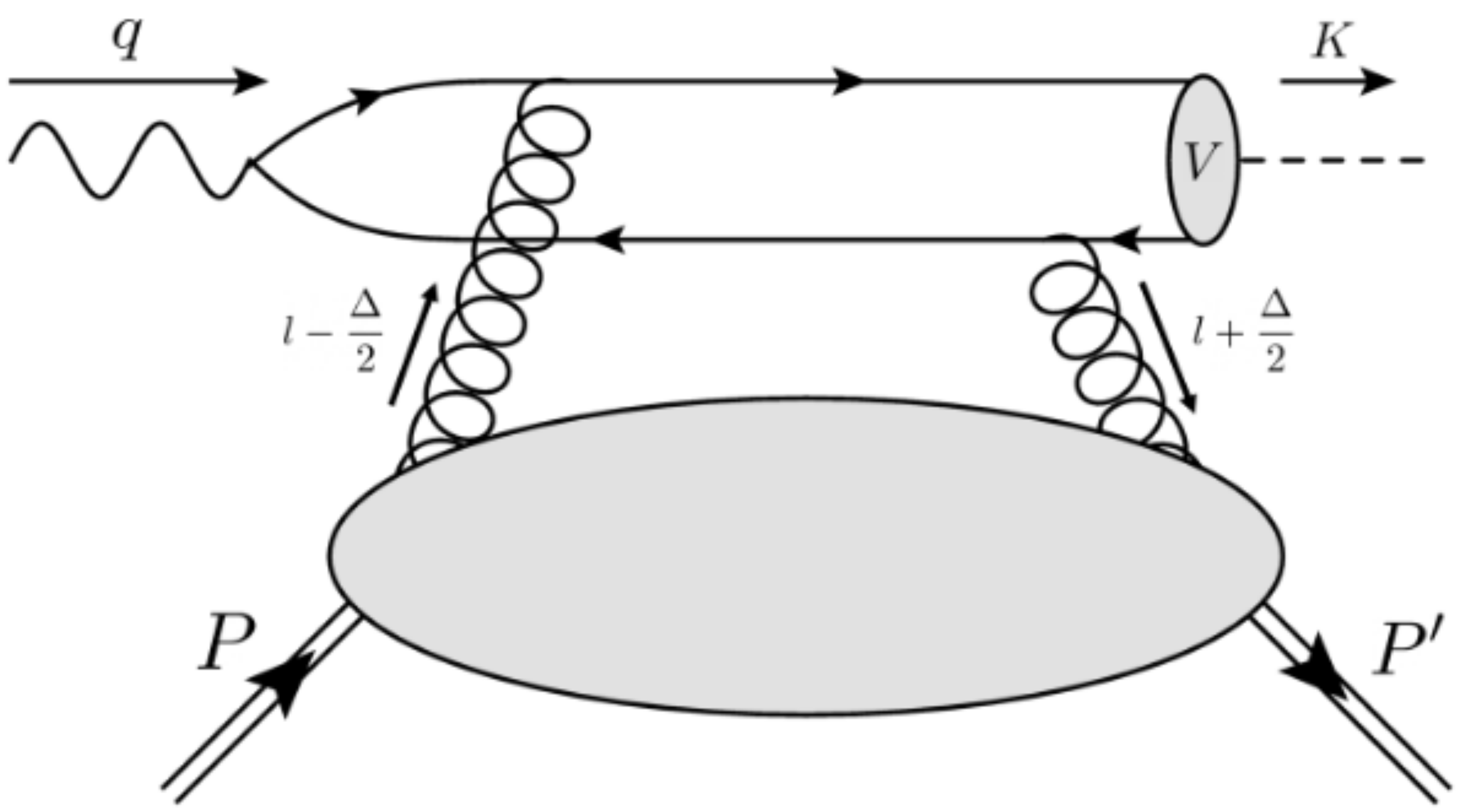

How does the GPD formalism change if spin-flip corrections are sizeable?

Spin density matrix elements (GlueX/CLAS)

Conserving

$$\mathcal{M}(\varepsilon_V, \varepsilon) = \frac{8\sqrt{2}\pi\alpha_S(M_V)}{M_V^2}\phi^*(0)G(t,\xi)(\varepsilon_V^* \cdot \varepsilon)$$

Guo et al. [Phys.Rev.D 103 (2021) 9, 096010]

Violating

$$\langle \lambda_\gamma, \lambda_p | T | \lambda, \lambda_{p'} \rangle =$$

$$F(s,t) \times (\bar{u}\gamma_\mu u)\left[\epsilon_\gamma^\mu (q \cdot \epsilon_\psi^*) - (\epsilon_\gamma \cdot \epsilon_\psi^*) q^\mu\right]$$

JPAC [Phys. Rev. D 100, 034019 (2019)]

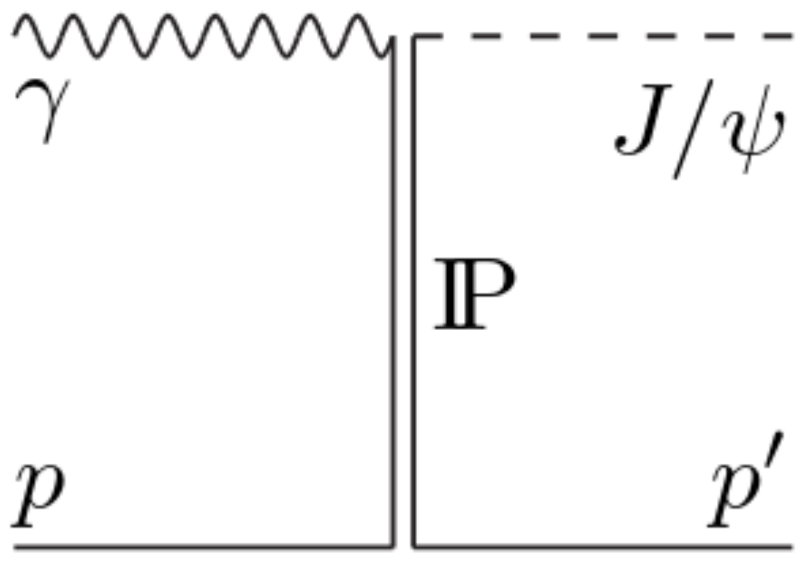

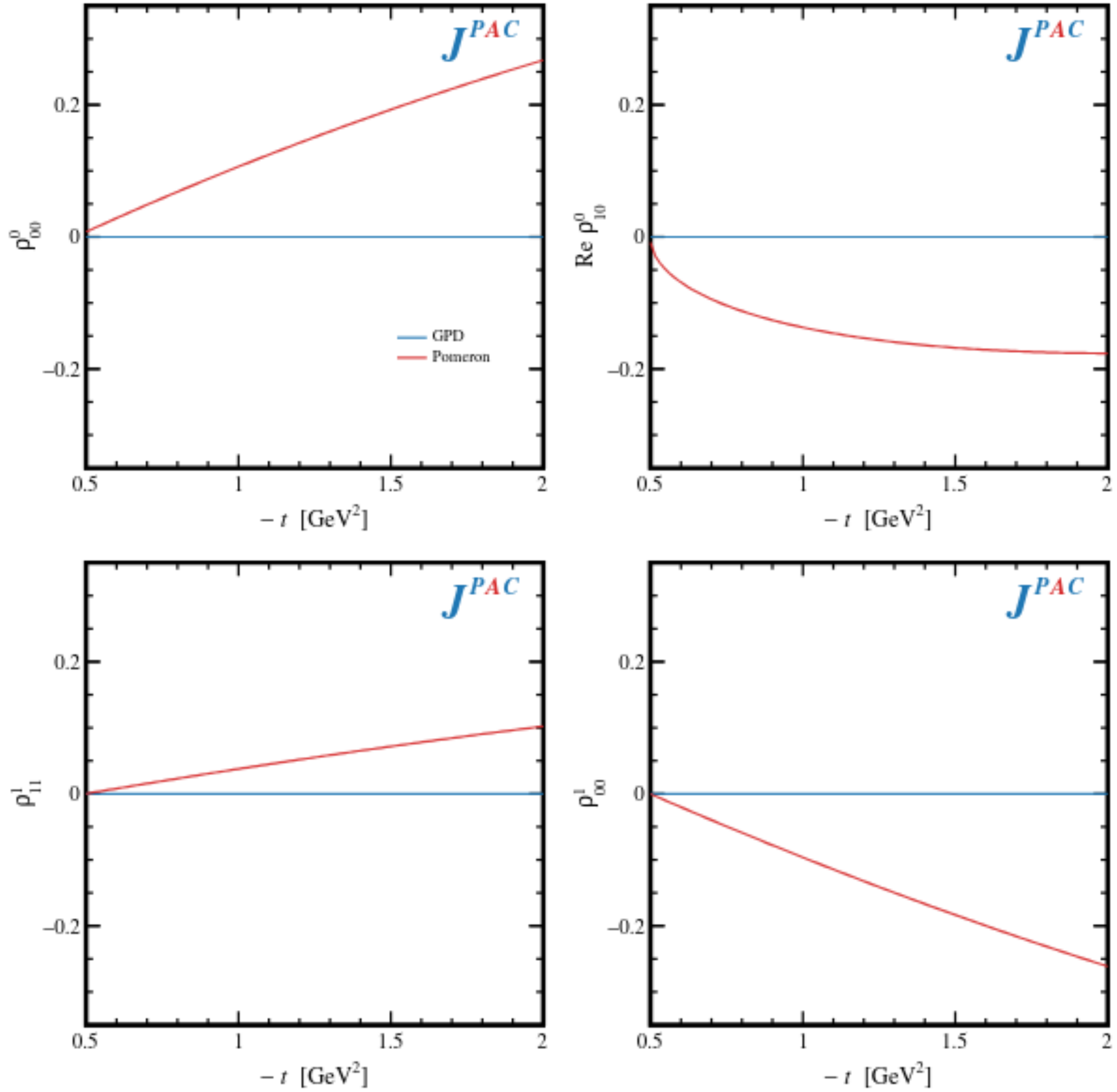

Conclusions

Accardi, et al. [EPJA 60 (2024) 163]

The underlying physics of the reaction is not certain

What physics can be extracted is not fully known

Open questions we <u>should not</u> ignore:

- Can we easily access the proton structure?
- Are there pentaquarks?
- Open charm contributions?
- Is VMD a good assumption?

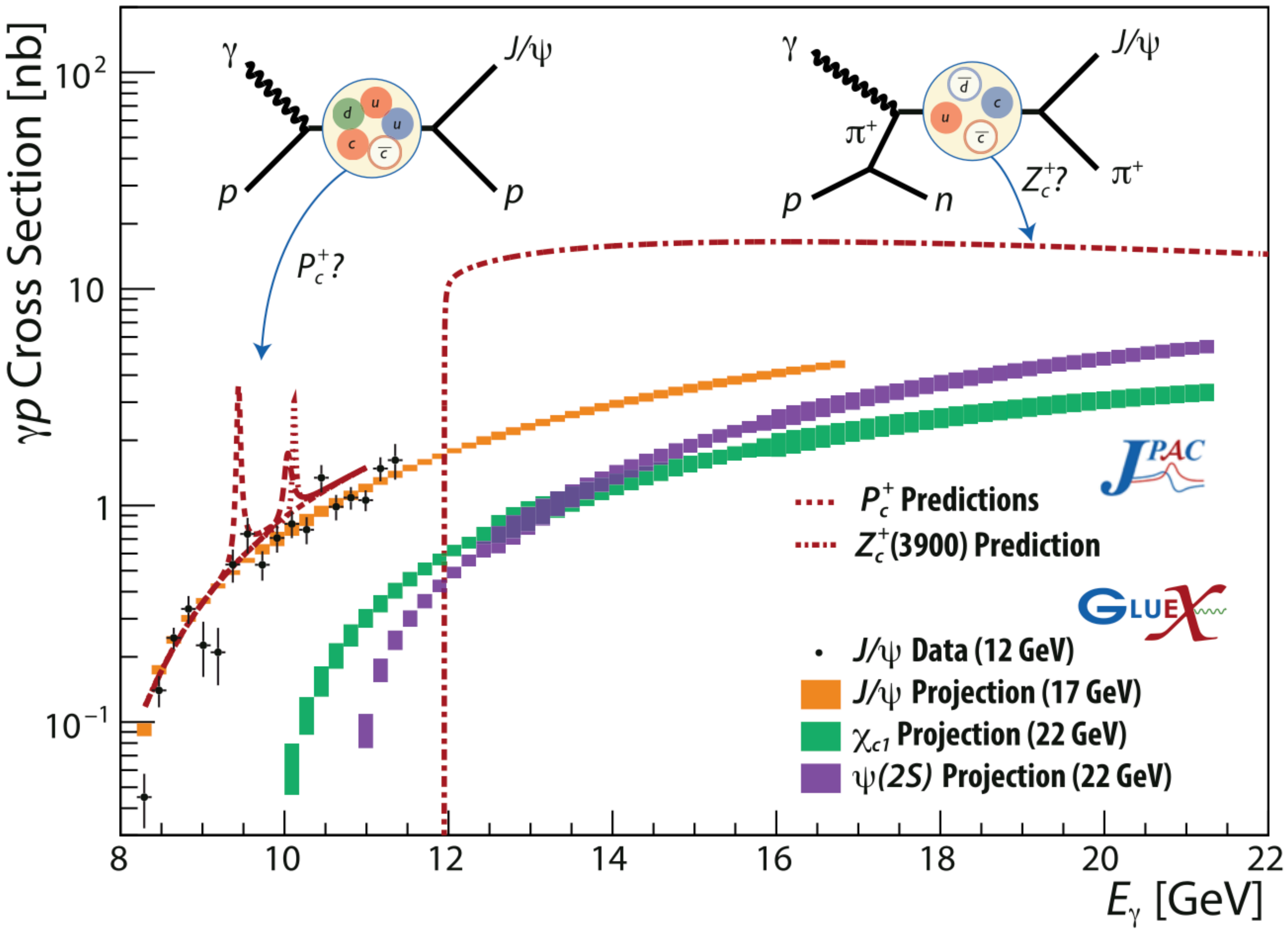

An important part of future facilities (EIC, EicC, JLab22) research program depends on answering to these questions

Spare slides

J/ψ photoproduction (high energy)

Historically J/ψ photoproduction has been well explored at high energies (W>20 GeV) at HERA

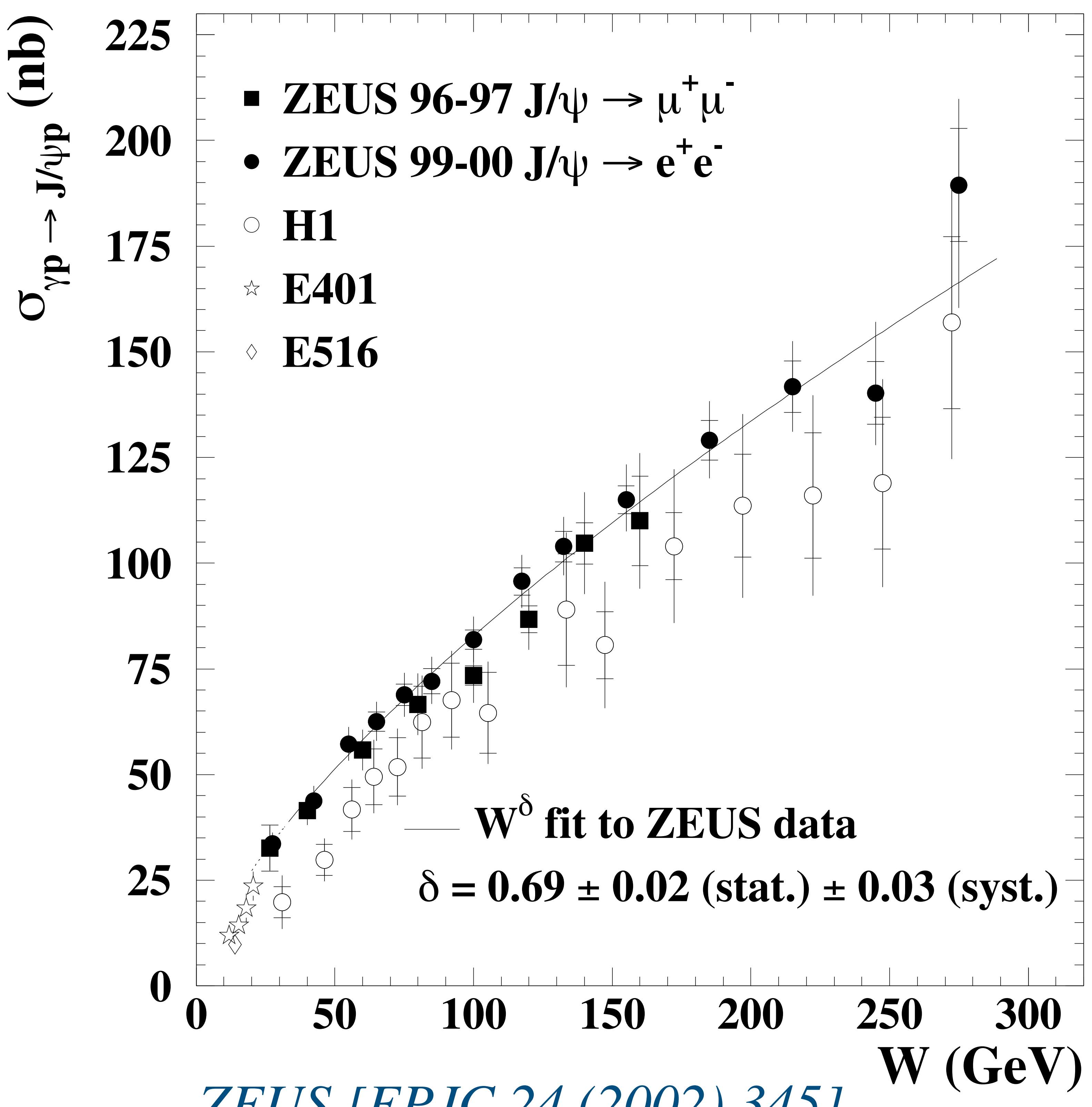

ZEUS [EPJC 24 (2002) 345]

Production dominated by low $|t|$ and exponential decay from forward angles — i.e. the "diffractive peak"

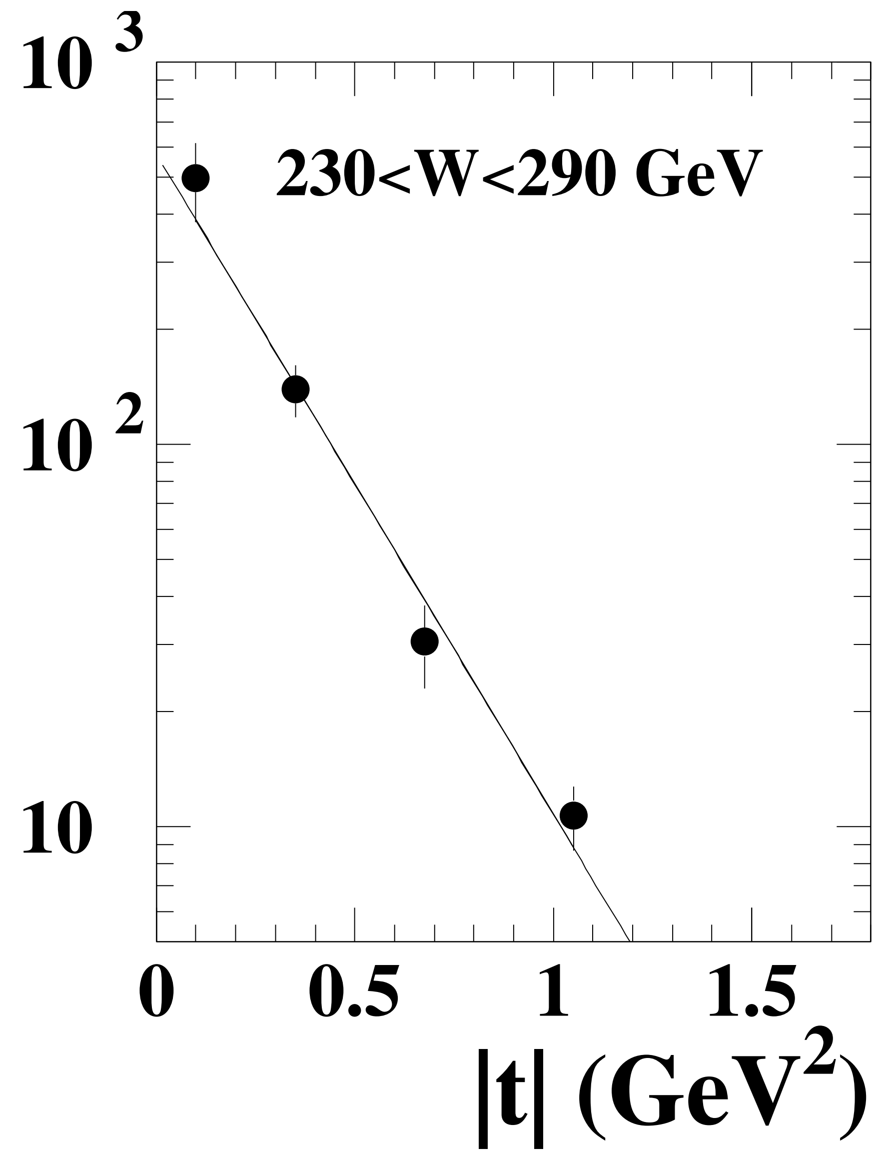

Diffractive production via gluon exchanges

Variety of theoretical models:

- Pomeron exchange

  Donnachie & Landshoff [PLB 437 (1998) 408]
- Color dipole

  Caldwell & Soares [NPA 696 (2001) 125]
- pQCD

  Ivanov et al. [EPJC 34 (2004) 297]

Differential cross section

Winney, et al. (JPAC) [PRD 108 (2023) 054018]
[Zenodo 8302620 (2023)]

The exponential t behavior is captured with <u>only a few partial waves</u>

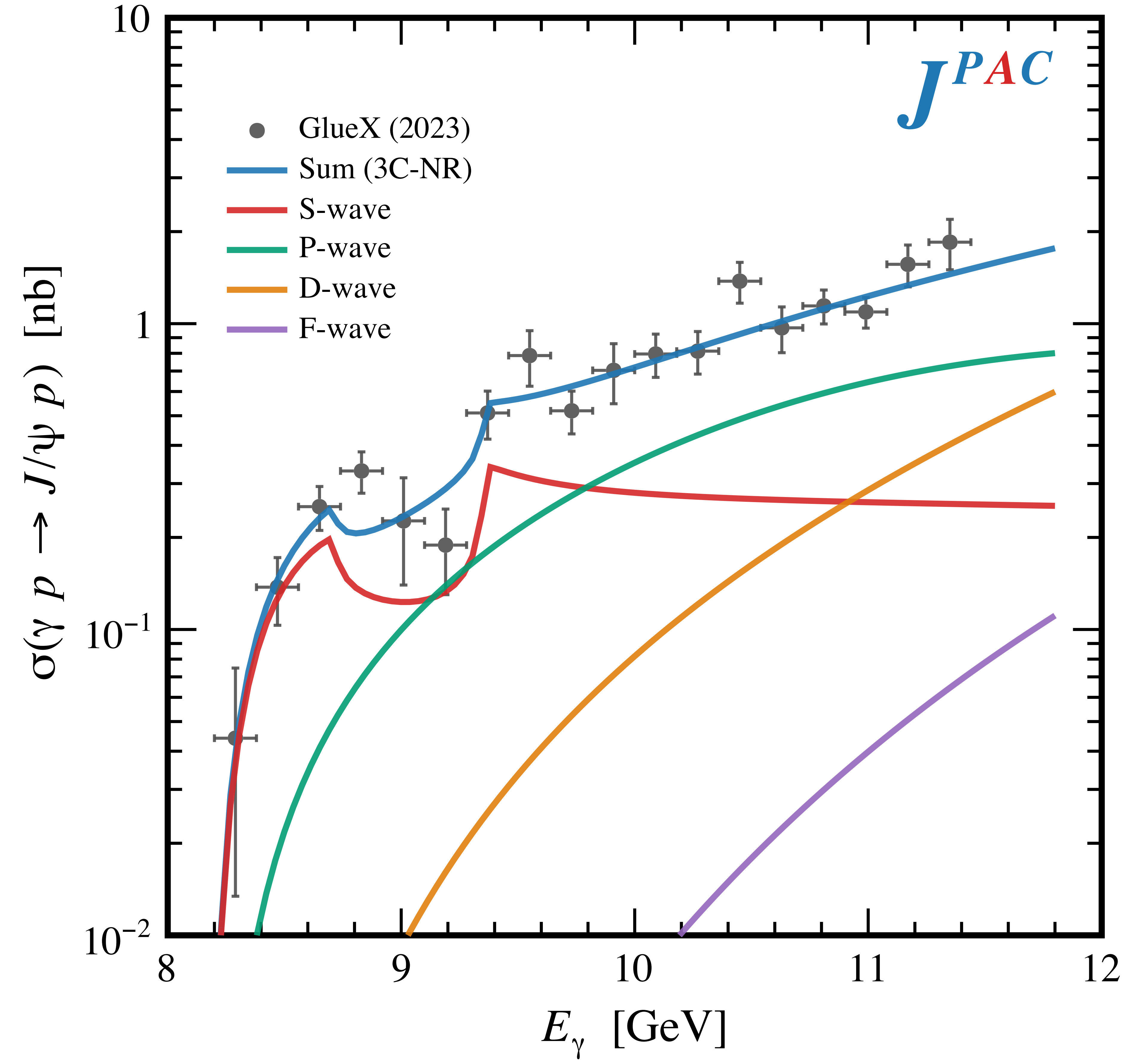

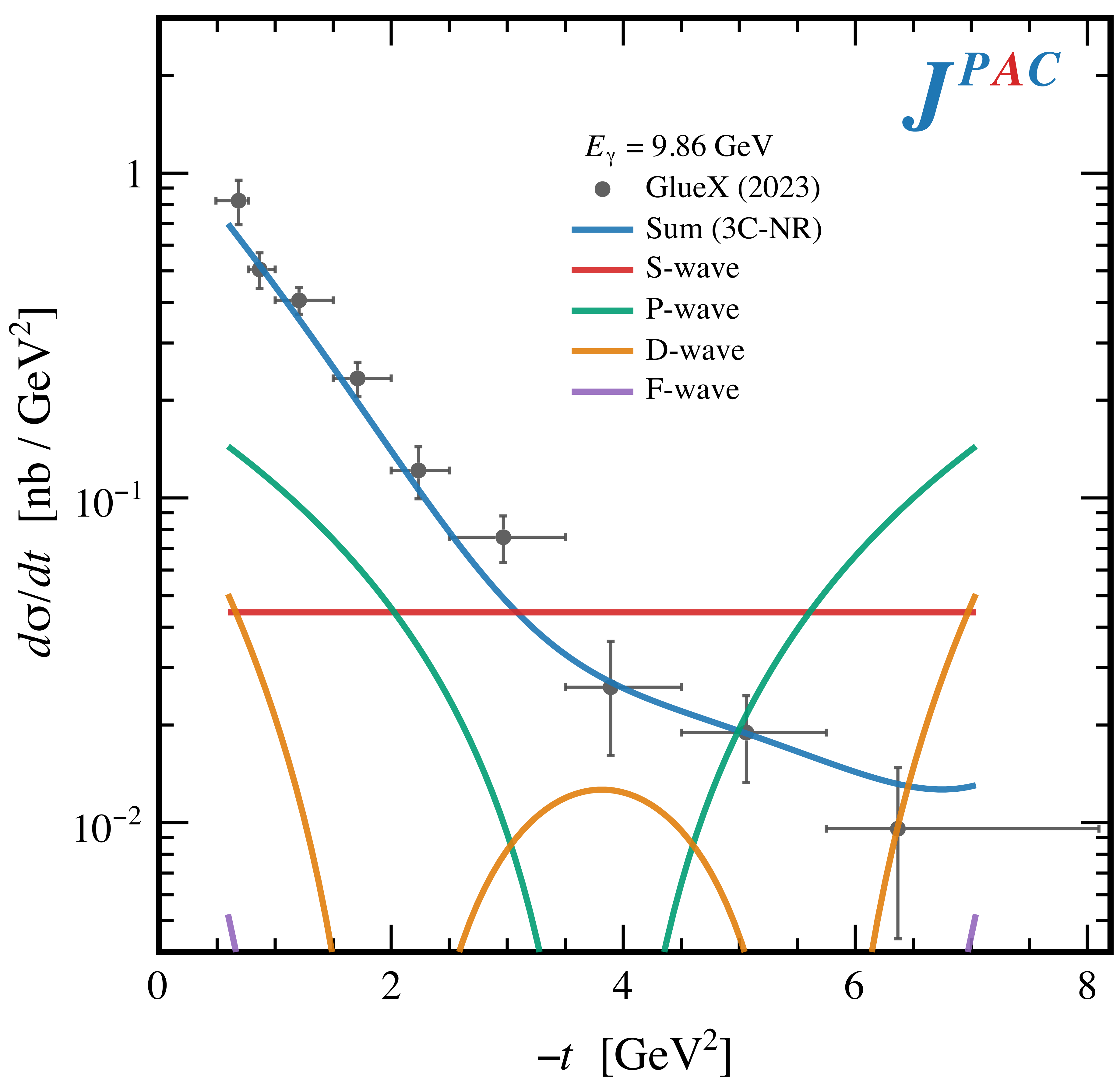

The sharp asymmetric t distribution is due to interference between PW: $P_\ell(\cos\theta = \pm 1) = (\pm 1)^\ell$

P-vector+K-matrix formulation

Winney, et al. (JPAC) [PRD 108 (2023) 054018]
[Zenodo 8302620 (2023)]

Limitations:

- Not a microscopic model
- Each partial wave must be parametrized independently

"Minimally model dependent, data driven analysis"

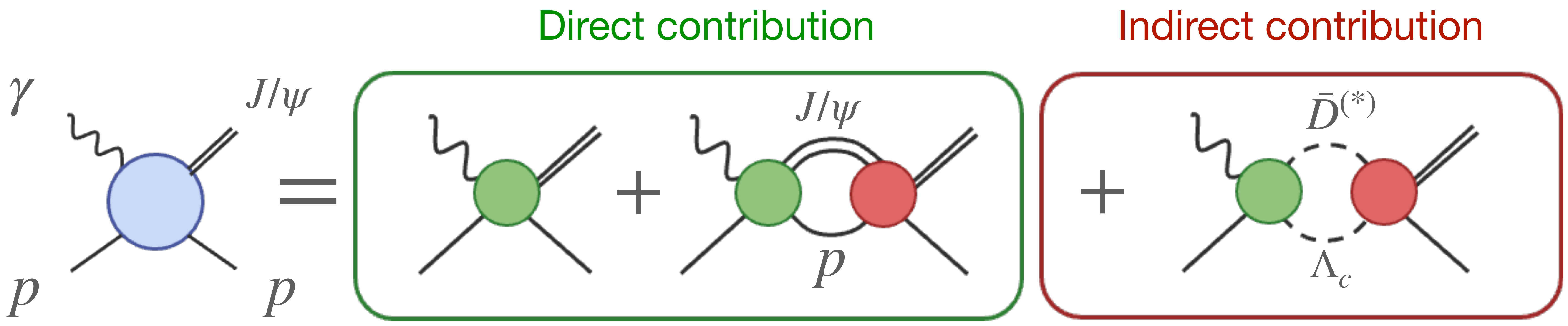

J/ψ photoproduction (near threshold)

Measurements at energies near threshold have attracted a lot of attention as potentitally sensitive to key quantities relevant to the nature of charmonium-nucleon interactions

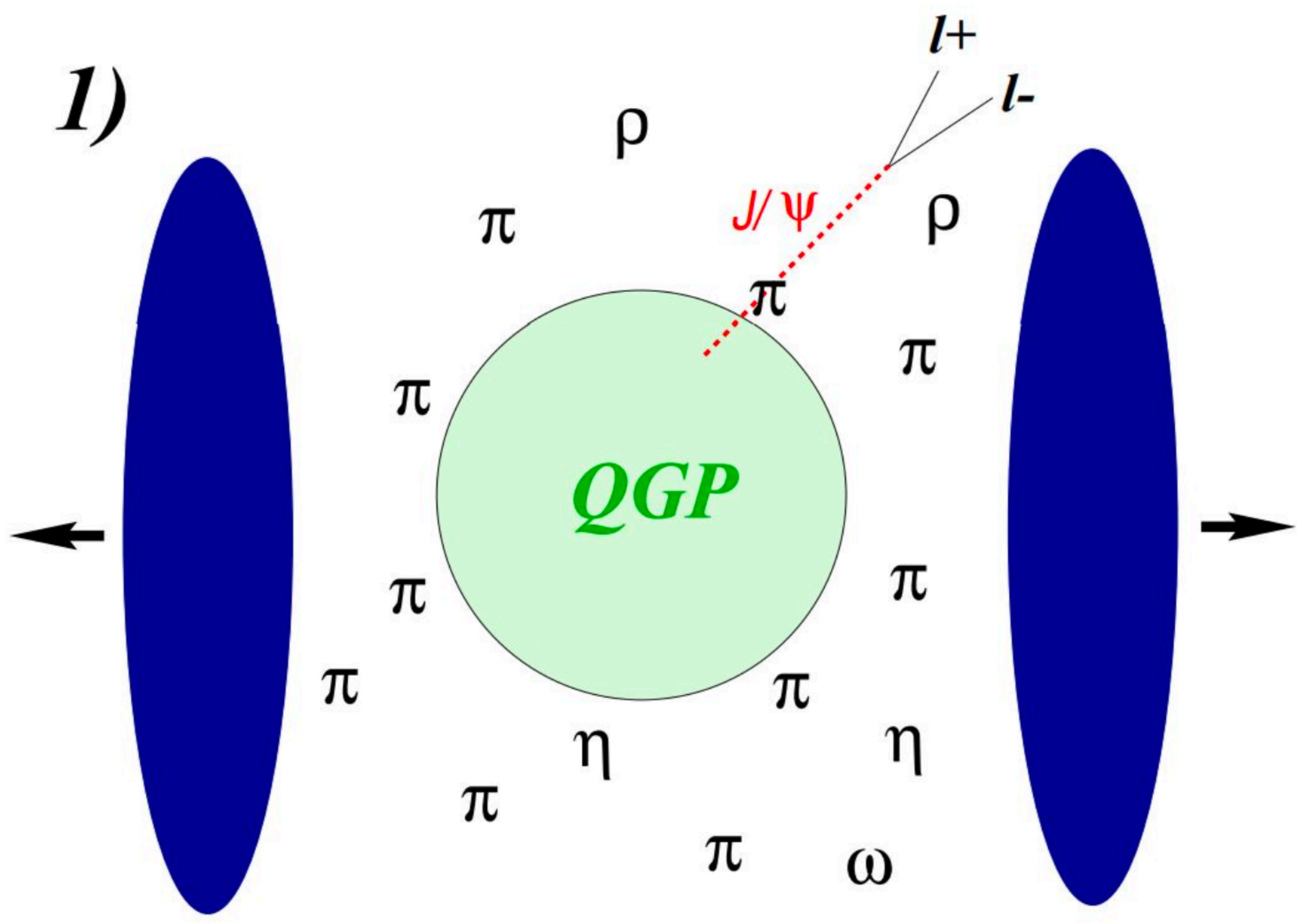

Near threshold, J/ψ-N interaction expected to be dominated by gluonic Van der Waals forces
Interaction predicted attractive and possibly strong enough to bind in nuclei

Brodsky & Miller [PLB 412 (1997) 125]
Brodsky, Schmidt & de Teramond [PRL 64 (1990) 1011]

Charmonium absorption cross sections are an important ingredient to search for quark-gluon plasma via charmonium suppression at heavy ion collisions

Barnes [Eur. Phys. J A 18 (2003) 531]
Matsui & Satz [PLB 178 (1986) 416]

Elastic scattering length

Extractions based on VMD consistent with nearly noninteracting system
First extraction without assuming VMD
Favors large values on the order of Fermi

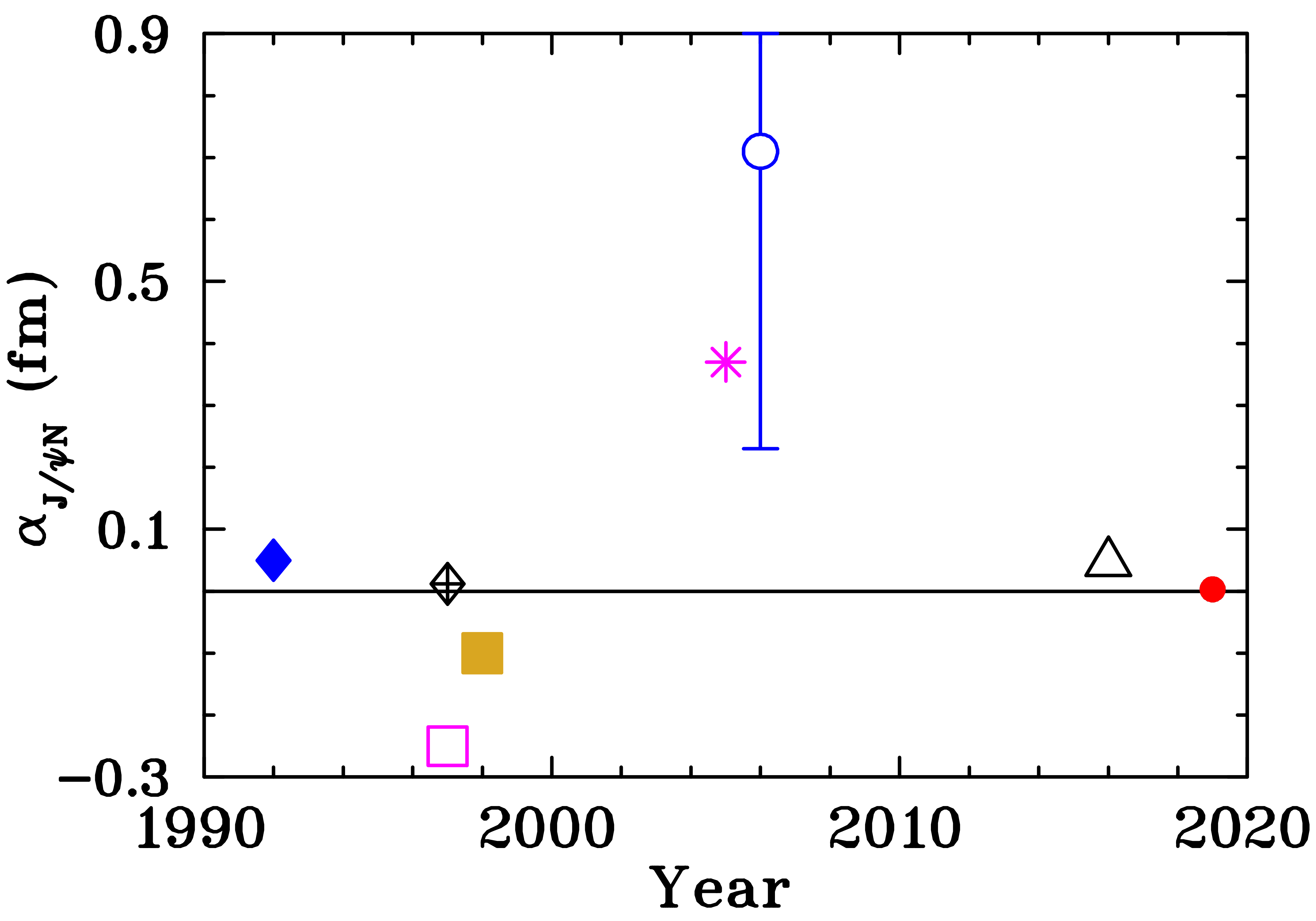

$$T_S^{\psi p,\psi p} = \frac{8\pi\sqrt{s_{\text{th}}}}{-a_{\psi p}^{-1} - iq} + \mathcal{O}(q^2)$$

Scattering length [fm]

1C	[0.56, 1.00]
2C	[0.11, 0.76]
3C-NR	[-2.77, 0.35]
3C-R	[-0.04, 0.19]

Typical hadronic interaction between nucleon and charmonia
3C fits are compatible with zero

Strakovsky, Epifanov & Pentchev. [PRC 101 (2020) 042201]

$|a_{\psi p}| = 3.08 \pm 0.55 \pm 0.45$ mfm   Using GlueX 2019 data

Charmonium-nucleon absorption

Charmonium absorption cross sections are an important ingredient to search for quark-gluon plasma via charmonium suppression at heavy ion collisions

$$\sigma_{tot}^{\psi p} = \frac{1}{2q\sqrt{s}} \mathrm{Im} T^{\psi p, \psi p}(s, t=0)$$

Barnes [EPJA 18 (2003) 531]
Matsui & Satz [PLB 178 (1986) 416]

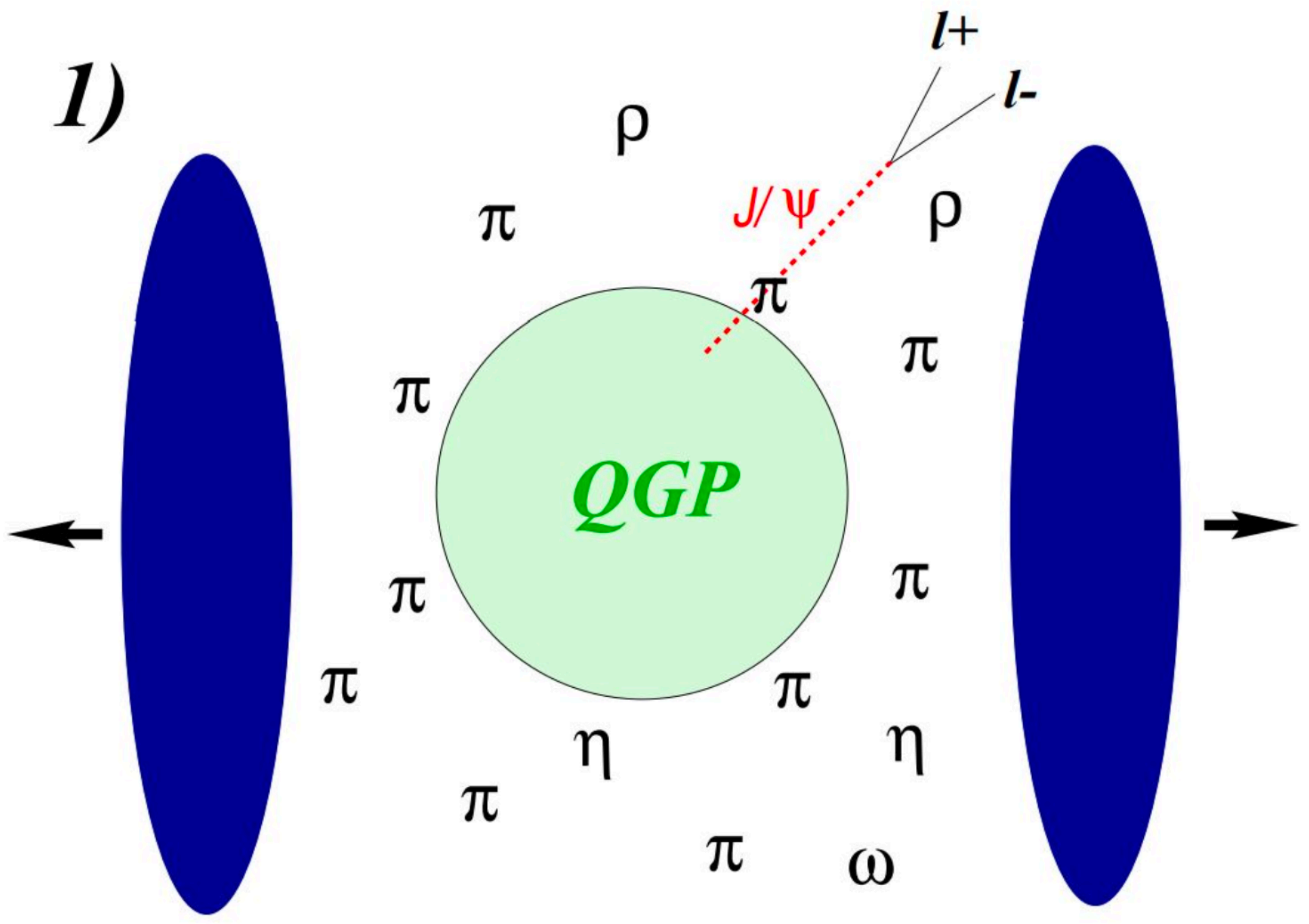

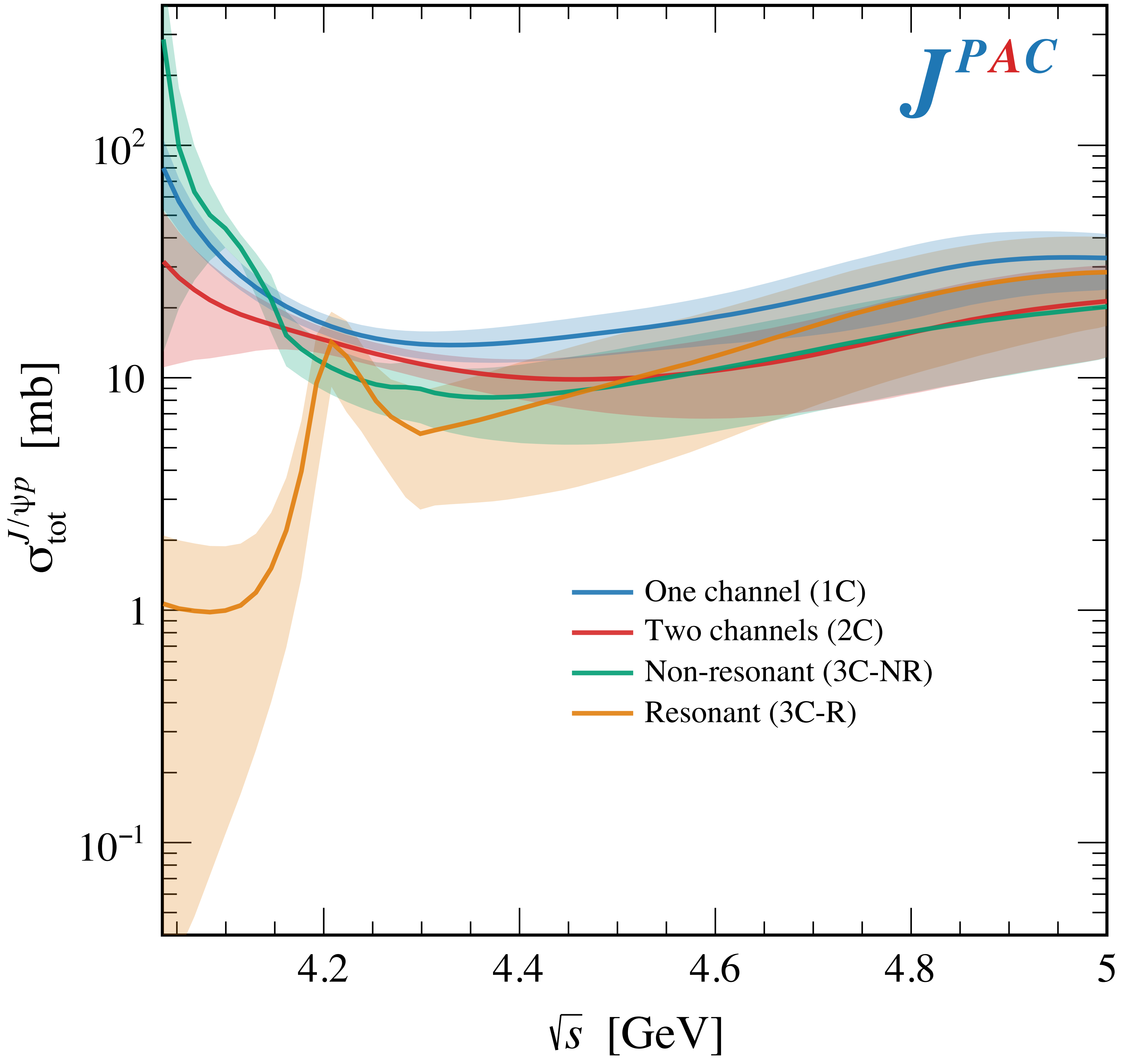

Vector meson dominance

VMD is used extensively in the phenomenology of photoproduction processes

Provides connection between production and elastic scattering

Works very well in the light mesons sector

Not clear if it also works in the heavy meson sector

It is hoped to provide reliable estimation of the order of magnitude

Explicit tests in heavy states near threshold has never been conducted

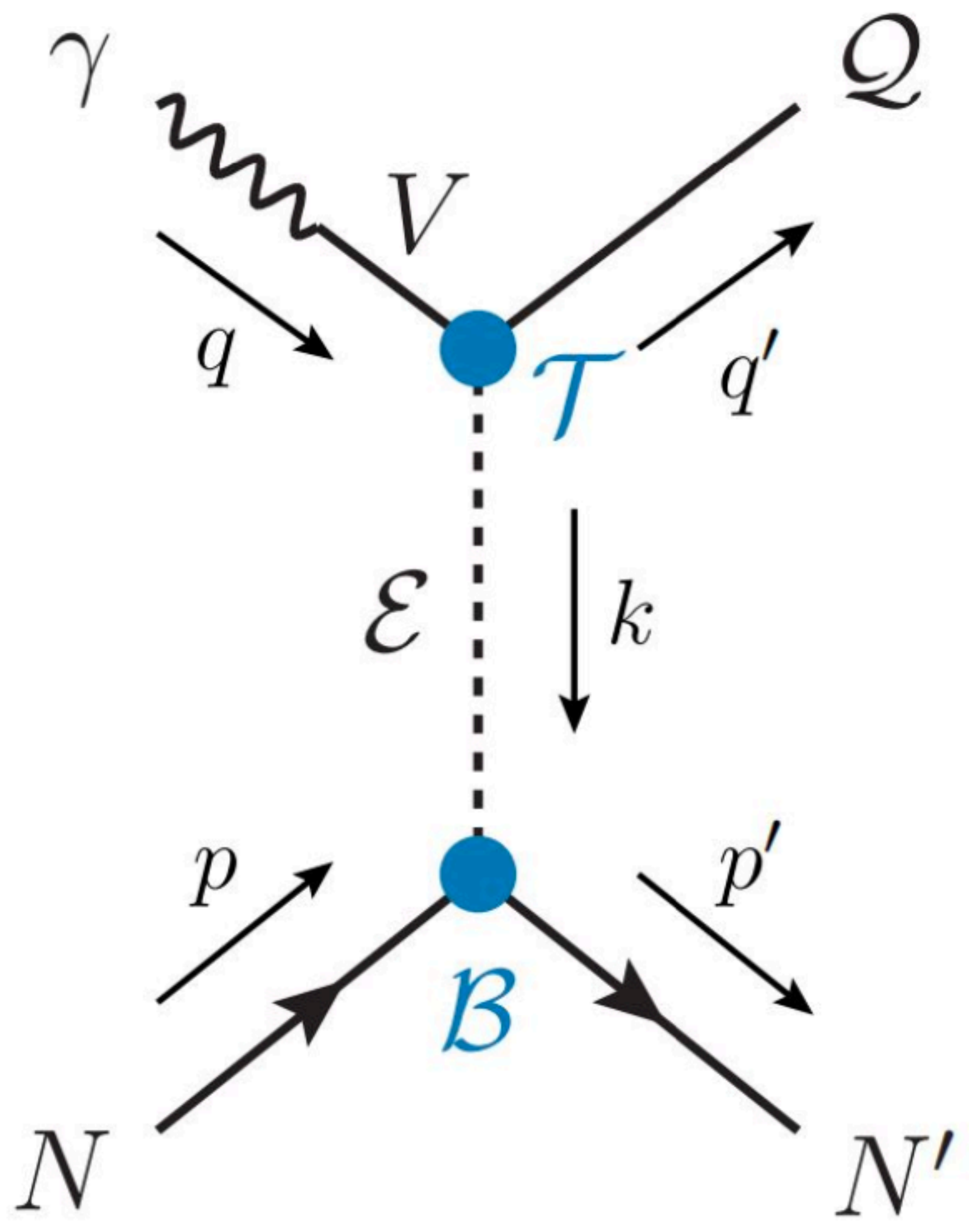

$F^{\psi p}(s,x) = g_{\gamma\psi} T^{\psi p,\psi p}(s,x)$ (strict VMD) $g_{\gamma\psi} = e f_\psi / m_\psi \simeq 0.0273$

$F_\ell(s) = f_\ell \left(1 + G T_\ell\right)$

Vector meson dominance

The K-matrix formalism allows us to extract the elastic J/ψ p amplitude from unitarity

We define the ratio to test the validity of the VMD assumption

$$R_{VMD}(x) = \left| \frac{F^{\psi p}(s_{th}, x)/g_{\gamma\psi}}{T^{\psi p, \psi p}(s_{th}, x)} \right|$$

	$x = \cos\theta = 0$	$x = t = 0$
1C	[0.45,0.73]×10^{-2}	[1.3,2.0]×10^{-2}
2C	[0.39,1.69]×10^{-2}	[1.3,5.1]×10^{-2}
3C-NR	[0.03,1.74]×10^{-2}	[0.08,8.9]×10^{-2}
3C-R	[1.4×10^{-2},0.58]	[5.4×10^{-2},1.8]

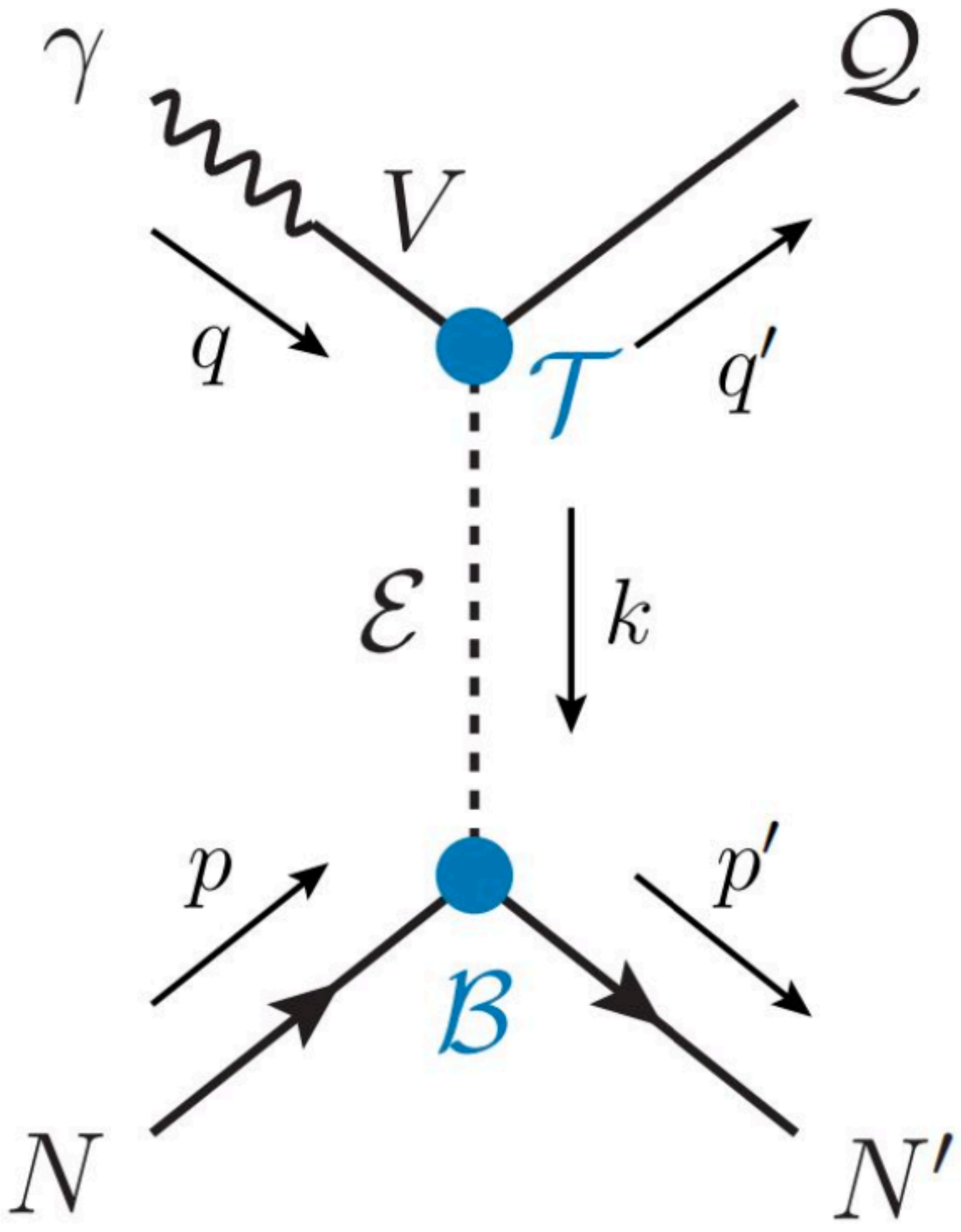

VMD found to underestimate elastic scattering by 2 orders of magnitude in all cases except those with a nearby pole

JLab22 GlueX

Accardi, et al. [EPJA 60 (2024) 163]

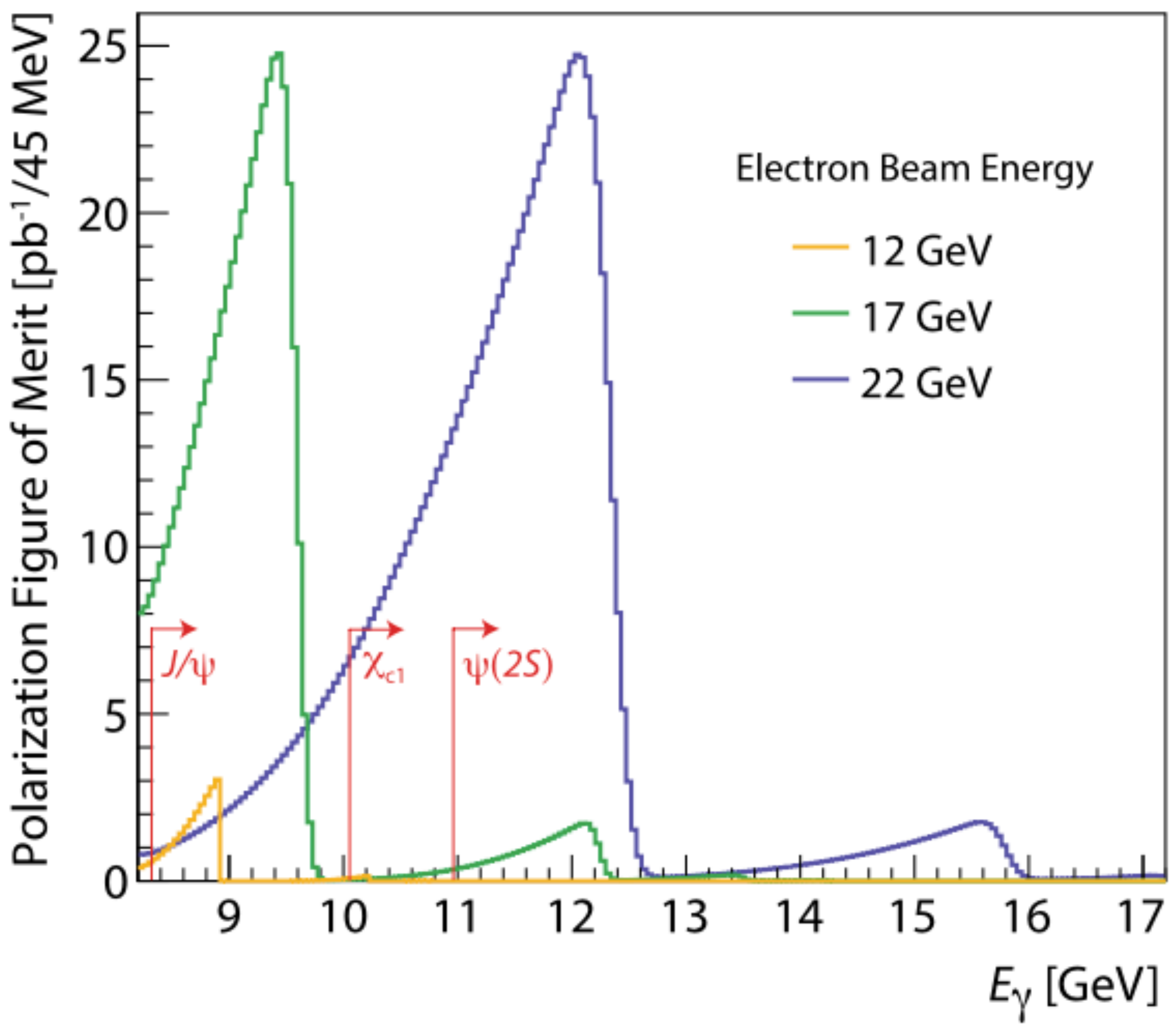

Fig. 5 The polarization figure of merit ($P^2(dN_\gamma/dE)$) as a function of photon beam energy E_γ for the existing 12 GeV GlueX configuration assuming 100 days of beam on target (yellow). Figures of merit assuming equal beam time are shown for 17 GeV and 22 GeV electrons, both of which are drawn for the same diamond orientation. Various $c\bar{c}$ production thresholds are shown

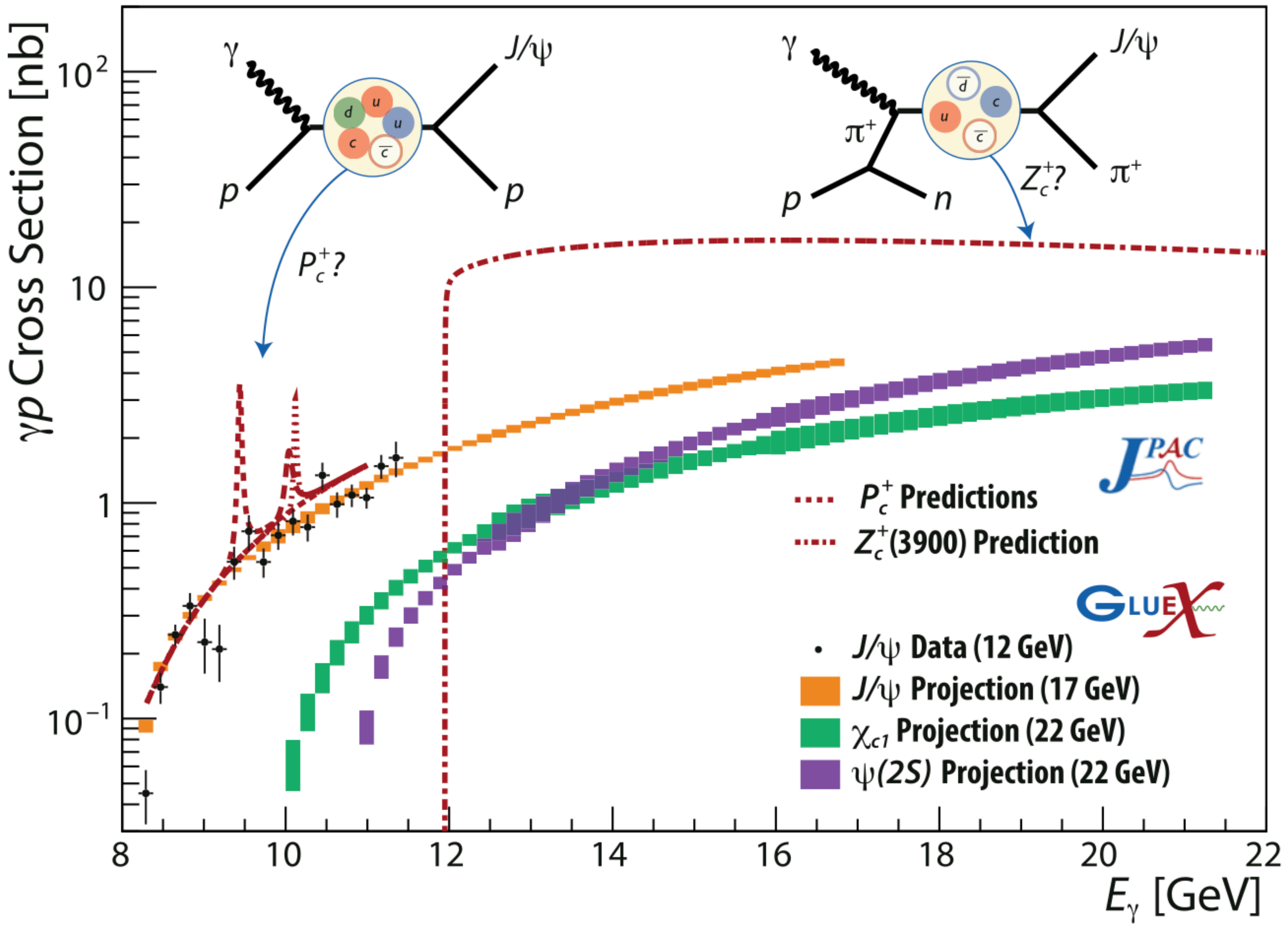

Fig. 3 Photoproduction cross sections of states containing $c\bar{c}$ as a function of photon beam energy. The points are GlueX data [21] The colored boxes are projections of statistical precision using the GlueX detector with different assumptions about the electron energy. The collection of dashed and dotted curves indicate how pentaquark P_c [22] or tetraquark Z_c [23] candidates might appear

Proton mass decomposition

Not without controversy:

Ji [PRL 74 (1995) 1071, PRD 52 (1995) 271]

Lorcé [EPJC 78 (2018) 120]

Normal gluon energy contribution (from traceless part)

Quark mass term

$$M = M_q + M_g + M_m + M_a$$

Quark and antiquark kinetic and potential energies

Gluon energy contribution from the trace anomaly (from trace part)

Convergence of the partial waves

$$r^{2\ell} \equiv \lim_{s \to s_{th}} \left| \frac{F_\ell(s)/(pq)^\ell}{F_S(s)} \right|$$

If $pqr^2 < 1$ we may expect subsequent waves to be suppressed
For all the fits $r \simeq 0.1$ fm

Estimated breakdown at 14 GeV

Analytic continuation of the phase space

$$G_i = \frac{s - s_i}{\pi} \int_{s_i}^{\infty} ds' \frac{\rho_i(s')}{(s' - s_i)(s' - s)} = -\frac{1}{\pi} \left[\rho_i \log \left(\frac{\xi_i + \rho_i}{\xi_i - \rho_i} \right) - \xi_i \frac{m_{2i} - m_{1i}}{m_{2i} + m_{1i}} \log \frac{m_{2i}}{m_{1i}} \right]$$

skewness

$$\xi = \frac{P^+ - P'^+}{P^+ + P'^+} \simeq 1 + \mathcal{O}\left(\frac{M_V}{M_N}\right)$$

Guo, Ji & Liu [PRD 103 (2021) 096010]

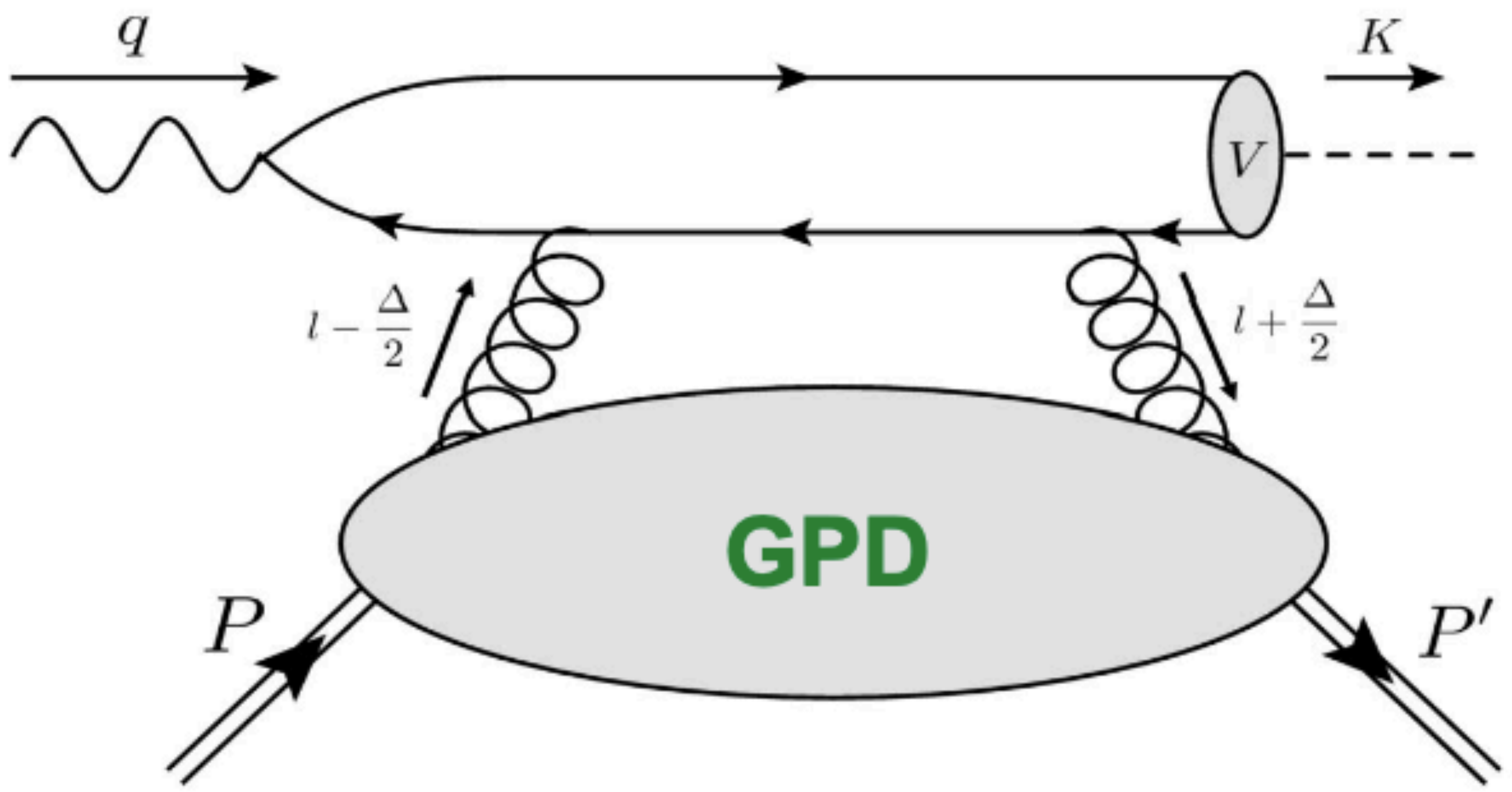

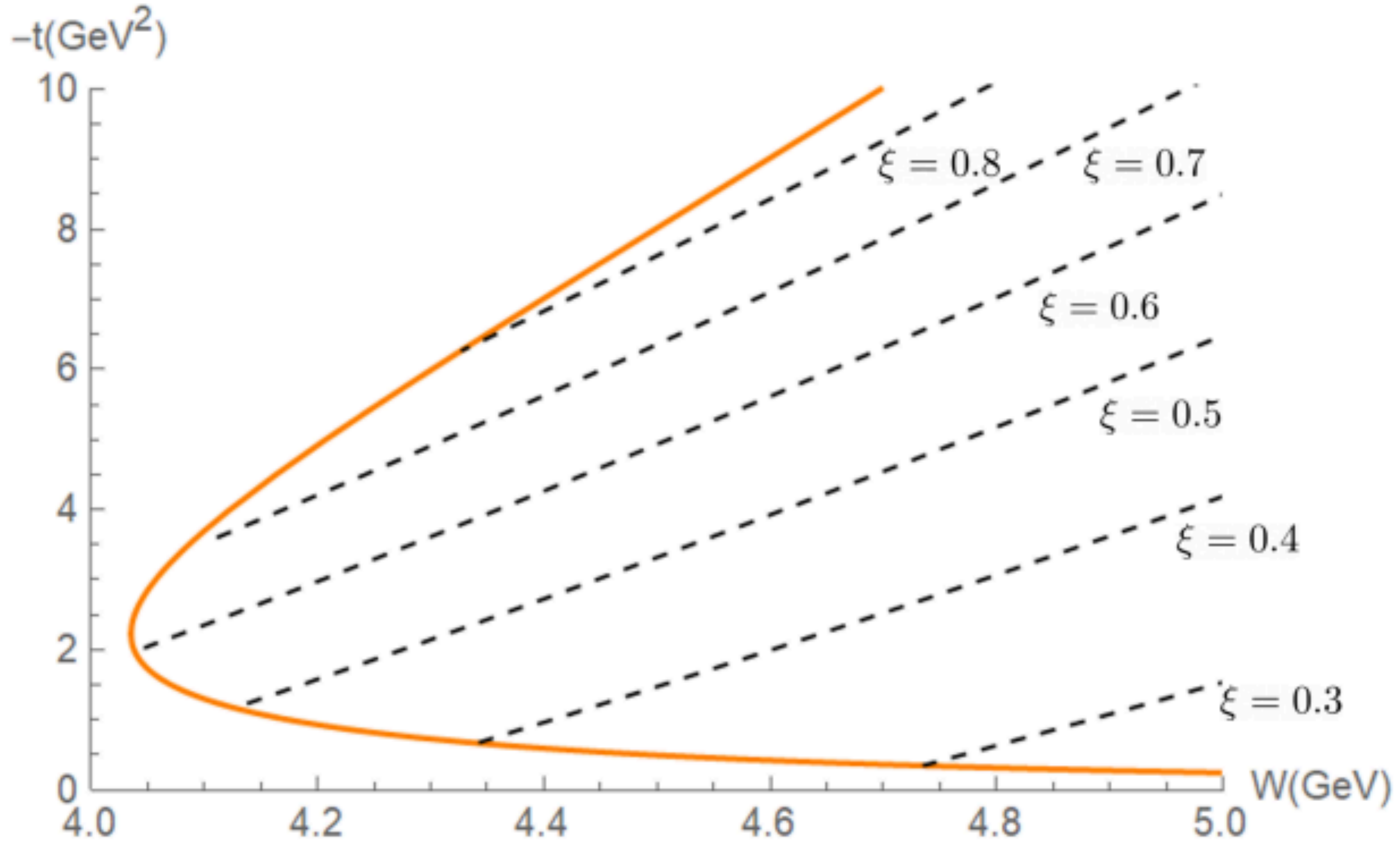

FIG. 2: ξ on the $(W, -t)$ plane in the kinematically allowed region with $M_{J/\psi} = 3.097$ GeV.